Thread based wearable electrochemical sensor for uric acid detection

Miss Kanyapat Teekayupak

จุฬาลงกรณ์มหาวิทยาลัย
CHULALONGKORN UNIVERSITY

A Thesis Submitted in Partial Fulfillment of the Requirements

for the Degree of Master of Science in Chemistry

Department of Chemistry

FACULTY OF SCIENCE

Chulalongkorn University

Academic Year 2019

ตัวรับรู้ทางเคมีไฟฟ้าสำหรับสวมใส่ฐานเส้นด้ายเพื่อการตรวจวัดกรดยูริก

น.ส.กัญญาพัชร ทีฆายุพรรค

จุฬาลงกรณ์มหาวิทยาลัย
CHULALONGKORN UNIVERSITY

Thesis Title   Thread based wearable electrochemical sensor for uric
                         acid detection
By   Miss Kanyapat Teekayupak
Field of Study   Chemistry
Thesis Advisor   Professor Dr. ORAWON CHAILAPAKUL
Thesis Co Advisor   Dr. NADNUDDA RODTHONGKUM

Accepted by the FACULTY OF SCIENCE, Chulalongkorn University in Partial Fulfillment of the Requirement for the Master of Science

.... Dean of the FACULTY OF SCIENCE
(Professor Dr. POLKIT SANGVANICH)

THESIS COMMITTEE

.... Chairman
(Associate Professor Dr. VUDHICHAI PARASUK)

.... Thesis Advisor
(Professor Dr. ORAWON CHAILAPAKUL)

.... Thesis Co-Advisor
(Dr. NADNUDDA RODTHONGKUM)

.... Examiner
(Associate Professor Dr. Narong Praphairaksit)

.... Examiner
(Associate Professor Dr. NATTAYA NGAMROJANAVANICH)

.... External Examiner
(Assistant Professor Dr. Wijitar Dungchai)

กัญญาพัชร ทีฆายุพรรค : ตัวรับรู้ทางเคมีไฟฟ้าสำหรับสวมใส่ฐานเส้นด้ายเพื่อการ
ตรวจวัดกรดยูริก. (Thread based wearable electrochemical sensor for uric
acid detection) อ.ที่ปรึกษาหลัก : ศ. ดร.อรวรรณ ชัยลภากุล, อ.ที่ปรึกษาร่วม : ดร.
นาฏนัดดา รอดทองคำ

ตัวรับรู้ทางเคมีไฟฟ้าฐานเส้นด้ายรูปแบบใหม่ถูกสร้างขึ้นอย่างประสบผลสำเร็จสำหรับการ
ตรวจวัดแบบไม่เจาะผ่านผิวหนังและไม่ใช้เอนไซม์ของกรดยูริกที่เป็นสารบ่งชี้ทางชีวภาพของโรคเก๊าท์ ใน
งานนี้ขั้วไฟฟ้าใช้งานถูกเตรียมโดยการเคลือบหมึกคาร์บอนบนเส้นด้ายเพื่อสร้างคุณสมบัตินำไฟฟ้า ตาม
ด้วยการดัดแปรขั้วไฟฟ้าด้วยอนุภาคนาโนทองคำเพื่อเพิ่มพื้นที่ผิวขั้วไฟฟ้าและการนำไฟฟ้า ลักษณะทาง
สัณฐานวิทยาของขั้วไฟฟ้าดัดแปรถูกแสดงลักษณะด้วยกล้องจุลทรรศน์อิเล็กตรอนแบบส่องกราดและ
อุปกรณ์วิเคราะห์ธาตุ ยืนยันว่าอนุภาคนาโนทองคำถูกดัดแปรบนผิวขั้วไฟฟ้า และพื้นที่ผิวของขั้วไฟฟ้าดัด
แปรเพิ่มขึ้น ลักษณะเฉพาะทางเคมีไฟฟ้าถูกศึกษาเช่นกันโดยใช้ไซคลิกโวลแทมเมตรีและดิฟเฟอเรนเชียล
พัลส์โวลแทมเมตรี แสดงว่าขั้วไฟฟ้าดัดแปรให้สัญญาณทางเคมีไฟฟ้าโดยประมาณ 2 เท่าสูงกว่าขั้วไฟฟ้าที่
ไม่ดัดแปร ภายใต้สภาวะที่เหมาะสม ตัวรับรู้ฐานเส้นด้ายดัดแปรแสดงการตรวจวัดกรดยูริกด้วยช่วงความ
เป็นเส้นตรง 0.01 ถึง 5.0 มิลลิโมลาร์และขีดจำกัดของการตรวจวัด 0.12 ไมโครโมลาร์ นอกจากนี้ตัวรับรู้
ดัดแปรถูกศึกษาว่าปราศจากการรบกวนจากสารรบกวนทั่วไปและสามารถถูกเก็บไว้เป็นระยะ 30 วันโดย
ไม่สูญเสียประสิทธิภาพ ท้ายที่สุดตัวรับรู้ฐานเส้นด้ายดัดแปรนี้ได้ถูกนำไปประยุกต์อย่างมีประสิทธิภาพ
สำหรับการตรวจวัดกรดยูริกในตัวอย่างปัสสาวะมนุษย์ และผลการทดลองที่ได้ถูกตรวจสอบโดย
เปรียบเทียบกับแมสสเปกโตรเมตรีซึ่งเป็นวิธีมาตรฐาน

จุฬาลงกรณ์มหาวิทยาลัย
CHULALONGKORN UNIVERSITY

สาขาวิชา	เคมี	ลายมือชื่อนิสิต	....
ปีการศึกษา	2562	ลายมือชื่อ อ.ที่ปรึกษาหลัก	....
		ลายมือชื่อ อ.ที่ปรึกษาร่วม	....

6072018923 : MAJOR CHEMISTRY

KEYWORD: Thread-based electrochemical sensor, Non-invasive sensor, Non-enzymatic, Gold nanoparticles, Uric acid

Kanyapat Teekayupak : Thread based wearable electrochemical sensor for uric acid detection. Advisor: Prof. Dr. ORAWON CHAILAPAKUL Co-advisor: Dr. NADNUDDA RODTHONGKUM

Novel cotton thread-based electrochemical sensor was successfully fabricated for a non-invasive and non-enzymatic detection of uric acid (UA), a biomarker of gout disease. In this work, the working electrode was prepared by coating a carbon ink on the cotton thread to create the conductive property, followed by electrode modification using gold nanoparticles (AuNPs) to increase electrode surface area and conductivity. The morphologies of the modified electrode were characterized by scanning electron microscopy (SEM) with energy dispersive X-rays spectroscopy (EDX), confirming that AuNPs were modified on the electrode surface and the surface area of the modified electrode increased. The electrochemical characteristics were also studied using cyclic voltammetry (CV) and differential pulse voltammetry (DPV), indicating that the modified electrode provided approximately 2 times higher electrochemical signals than an unmodified electrode. Under the optimal conditions, the modified cotton thread-based sensor exhibited the detection of UA with a linear range of 0.01-5.0 mM and a limit of detection (LOD) of 0.12 µM. Moreover, the modified sensor was investigated to be interferent free from common interfering substances and could be stored for 30 days without efficiency loss. Ultimately, this modified cotton thread-based sensor was effectively applied for the determination of UA in human urine sample and the obtained results were validated by comparing with mass spectrometry as a standard method.

Field of Study:	Chemistry	Student's Signature	....
Academic Year:	2019	Advisor's Signature	....
		Co-advisor's Signature	....

ACKNOWLEDGEMENTS

TABLE OF CONTENTS

LIST OF FIGURES

LIST OF TABLES

จุฬาลงกรณ์มหาวิทยาลัย
CHULALONGKORN UNIVERSITY

CHAPTER I

INTRODUCTION

1.1 Introduction

Non-invasive diagnosis has gained considerable attention in recent years because it can be used as an alternative blood-free diagnosis approach to directly detect the target biomarkers excreted from human body fluids without the painfulness and infection [1-4]. Among all substrates used as a non-invasive sensor, textile has become the most attractive material due to its biocompatibility, comfortability and stretch ability [5, 6]. However, the use of fabric textile substrates still requires high volume of biofluid sample leading to unsuitability for medical diagnosis which the sample volume is limited. To overcome this problem, the cotton thread has become an alternative one because it requires the low sample volume and provides self-microfluidic property for the flow of biofluid with low cost and commercial availability [7-12].

In case of a biomarker of interest, uric acid (UA), chemically designated as 2, 6, 8-tryhydroxypurine, is a major product of the catabolism of purine nucleosides, adenosine and guanosine in human's fluid. The existing level of UA in the fluids is an important biomarker for gout diagnosis [13]. It has been clinically reported that, gout is linked to an abnormal level of uric acid in human urine over 4.46 mM [14]. Generally, UA detection is performed by blood withdrawing using an invasive needle, which cause painfulness and high infection risk. Therefore, a non-invasive electrochemical sensor of UA in human urine was recently investigated for replacing of the traditional invasive diagnosis [15, 16].

Various analytical techniques, such as liquid chromatography (HPLC) [17], capillary electrophoresis (CE) [18], and fluorescence spectroscopy [19] have been reported for separation and detection of UA. However, the limitations of the above techniques are expensiveness, requirement of additional steps, specialist and complicated instrument. To overcome these drawbacks, an electrochemical sensor is an alternative approach, which is suitable for diverse applications due to its simple and rapid analysis, inherent miniaturization and inexpensiveness [20-22]. Therefore, the

electrochemical sensor was developed for a non-invasive diagnosis of biomarkers in urine to indicate the human's health status. Traditionally, the electrochemical sensor of UA was performed by an enzymatic platform using uricase enzyme [23-25]. Although this enzyme-based sensor provides high specificity and sensitivity, it still has some disadvantages, including high cost, operational complexity and enzymatic stability issue. Therefore, a non-enzymatic detection of UA is emerged through its oxidation on the modified electrodes offering low cost and more simplicity [26].

However, an important limitation of the non-enzymatic sensor on a small size of the cotton thread-based electrode is low surface area leading to decreased sensor sensitivity. To overcome this problem, modification of working electrode surface is highly required to enhance the electrode surface area for increasing of the sensor sensitivity. The metallic based nanoparticles have been used for electrode surface modification due to their high conductivity, high surface area, high mechanical strength, and electrocatalytic property [27-30].

In this work, a cotton thread-based electrochemical sensor is fabricated for non-invasive and non-enzymatic detection of UA. The cotton thread was coated with the conductive carbon ink and used as a working electrode. Then, gold nanoparticles (AuNPs) was electrodeposited on the surface of the working electrode to increase the electrode surface area and enhance the detection sensitivity for UA. After that, the modified cotton thread-based electrode was directly used as a working electrode for an electrochemical sensor of UA without the enzyme requirement. This sensor showed a high sensitivity towards UA detection with a wide linear range and it was applied for non-invasive and non-enzymatic sensor of UA in human urine sample.

1.2 Objectives

- To fabricate novel cotton thread-based electrochemical sensor modified with gold nanoparticles
- To apply the modified cotton thread-based electrochemical sensor for uric acid detection in urine

1.3 Scope of the research

In this study, the modified cotton thread-based electrochemical sensor was developed for the determination of uric acid (UA). The surface morphologies of the

modified cotton thread-based electrodes were systematically characterized. All factors affecting the analytical performances and sensitivities were optimized. Moreover, the analytical performances of the modified cotton thread-based sensors for electrochemical detection including a linear range, a detection limit and stability were evaluated. Under the optimized conditions, this cotton thread-based sensor was applied for the determination of uric acid in urine.

จุฬาลงกรณ์มหาวิทยาลัย
CHULALONGKORN UNIVERSITY

CHAPTER II

THEORY AND LITERATURE SURVEYS

In this chapter, the basic theory and principle of electrochemical techniques are described in the first part. In the second part, the surface electrode surface using nanomaterials is explained. Non-invasive sensor and substrate used for non-invasive sensor are introduced in the third part. Finally, the electrochemical detection of uric acid is discussed.

2.1 Electrochemical Methods

2.1.1 Principle of electrochemical methods [31, 32]

Electrochemistry is a study about the interaction between chemical reaction and electrical energy which is called the electrochemical reaction. This reaction focuses on the change of electron transportation process generated from target analyte reactions. The electrochemical technique has been extensively used for sensor for both quantitative and qualitative analyses. This technique has been widely used in various fields including medical diagnosis, environmental monitoring and food quality control.

Electrochemical methods are the analytical technique operated in an electrochemical cell that the concentration of target analytes can be evaluated by applying potential signal and measuring of the electrical parameter, for example, potential (volt; V) or current signal (amperes; A). These methods can be divided into two categories including potentiometric and potentiostatic methods (Figure 2.1)

interfacial
electrochemical techniques

static techniques
($i = 0$)

dynamic techniques
($i \neq 0$)

potentiometry
measure E

controlled
potential

controlled
current

variable
potential

fixed
potential

controlled-current
coulometry
measure i vs. t

amperometry
measure i

controlled-potential
coulometry
measure i vs. t

stirred
solution

quiescent
solution

stripping
voltammetry
measure i vs. E

hydrodynamic
voltammetry
measure i vs. E

linear potential
polarography and
stationary electrode
voltammetry
measure i vs. E

pulsed potential
pulse polarography
and voltammetry
measure i vs. E

cyclical potential
cyclic
voltammetry
measure i vs. E

Figure 2.1 The family tree of electrochemical techniques.

Potentiometric is a static technique (zero current) that measures the potential of a solution between the working and the reference electrode. The potential of working electrode depends on the concentration of analytes that can be calculated from the equation below.

$$E_{cell} = E_{ind} - E_{ref} + E_j$$

Where E_{cell} =   cell potential

E_{ind} =   potential of indicator electrode

E_{ref} =   potential of reference electrode

E_j =   junction potential

Potentiostatic technique is a dynamic technique (no zero current) that measures current response obtained from electron transfer process when a working electrode is applied with controlled potential and the results are plotted between applied potential and current called voltammogram. The applied potential can cause a redox reaction (oxidation and reduction) in the electroactive species of target analytes when an electron is received and lost between working electrode surface and solution (Figure 2.2). The current response obtained from potentiostatic technique is related to the concentration of target analytes in solution. The redox reaction of target analytes at electrode-solution interface is explained in an equation below.

$$O + ne^- \leftrightarrow R$$

Where O and R are the oxidized and reduced forms of electroactive species of target analytes, respectively. This redox reaction can occur when the system is applied with potential that makes electron transfer thermodynamically or kinetically. For the thermodynamic electron transfer process, the relationship between concentration of electroactive species of target analytes and applied potential can express as a Nernst equation that is shown in an equation below.

$$E = E^0 + \frac{2.3\,RT}{nF} log \frac{C_0(0,t)}{C_R(0,t)}$$

Where	E^0	=	standard potential of redox process
	R	=	gas constant (8.314 $JK^{-1}mol^{-1}$)
	T	=	Kelvin temperature
	n	=	number of transferred electrons
	F	=	Faraday constant (96,487 coulombs)
	C_0, C_R	=	concentration of oxidized species and reduced species, respectively
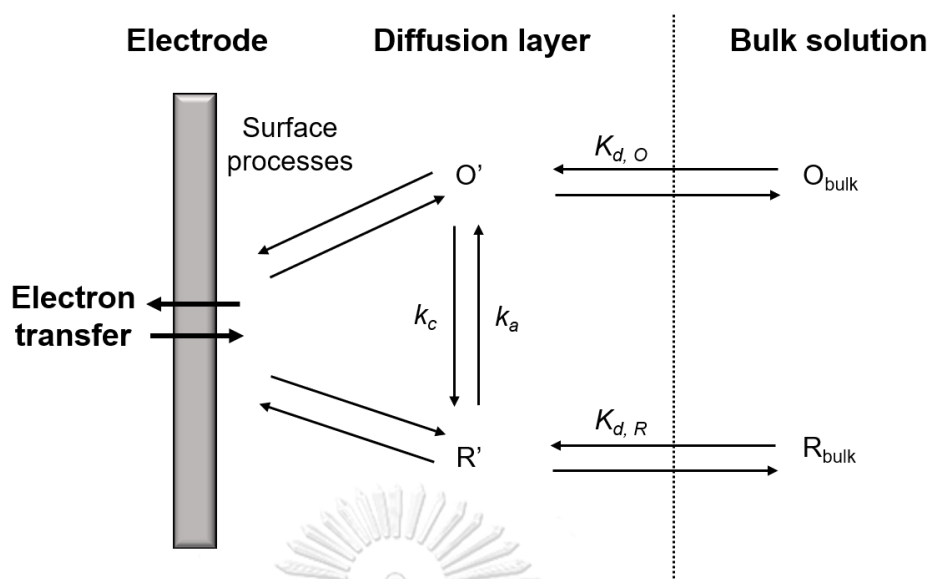
Figure 2.2 Schematic of the redox reaction at working electrode surface. [33]

For the electrochemical methods, the potentiostatic techniques including cyclic voltammetry (CV), differential pulse voltammetry (DPV) and amperometry, were selected for the detection of target analyte in this work. The basic principle of these techniques will be discussed in section 2.1.4, 2.1.5 and 2.1.6, respectively. Moreover, the surface property of the modified sensor was also characterized by electrochemical impedance spectroscopy (EIS). The basic principle of this technique will be discussed in section 2.1.7, accordingly.

2.1.2 Electrochemical cell

Generally, an electrochemical cell consists of three main components including external power supply, electrolyte and three-electrode system (working, reference and counter electrodes) as shown in Figure 2.3. The working electrode is used for the detection of target analyte. The reference electrode is a stable electrode that measures the potential of the working electrode without passing through of current. The counter electrode is also used to balance the current observed at the working electrode. To complete the circuit, this system is controlled by an external power supply and all of electrodes are immersed into an electrolyte solution containing target analyte as shown in Figure 2.3. To detect the target analytes, electrochemical cell containing three electrodes is used to measure the electrochemical changes of target analyte occurring when chemicals interact with the surface of the working

electrode. Previously, the conventional system of electrochemical cell is large that has a major drawback of the high sample volume requirement. To overcome this, the conventional system is miniaturized to a small and portable size called a screen-printed carbon electrode that is suitable for biomedical applications due to its requirement of low sample volume and field-based site measurement (Figure 2.4).
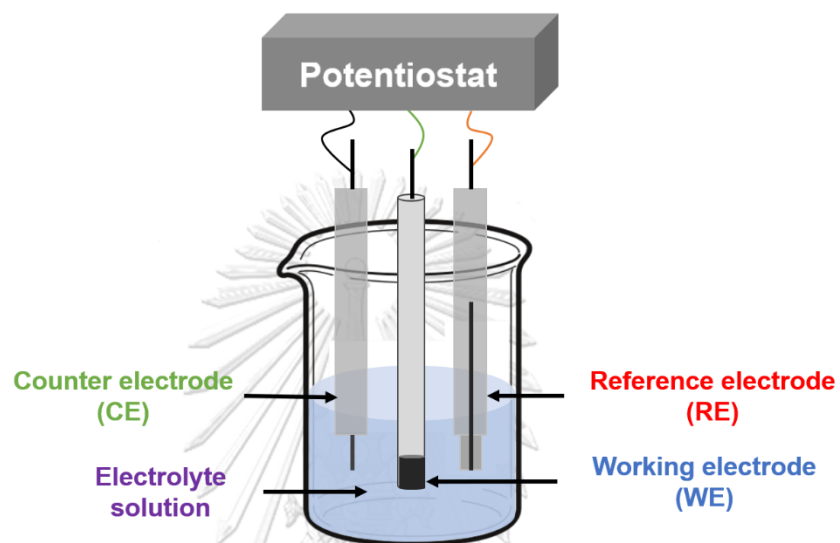
Figure 2.3 A conventional electrochemical cell.
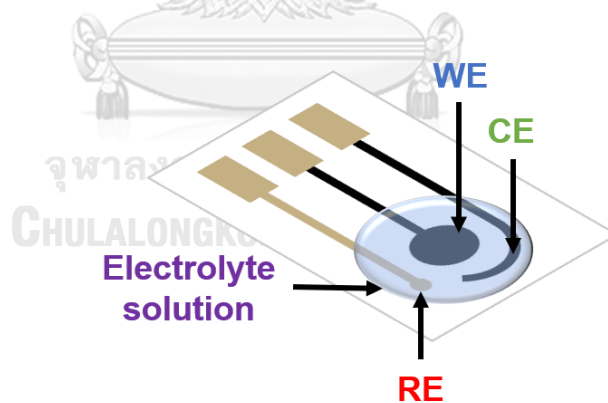
Figure 2.4 A screen-printed carbon electrode.

2.1.3 Mass transfer in electrochemical system

Mass transfer is the movement of target analytes in an electrolyte solution from one location to another. It can be moved from bulk solution to the working electrode surface under the control of electrical potential and different chemical conditions. Mass transport process can be described into three parts including diffusion mass transfer, migration mass transfer and convection mass transfer.

Diffusion is the random movement of molecules from high to lower concentration regions for one dimension as shown in Figure 2.5. The rate of different concentrations between two points in solution can be called concentration gradient. This movement under the influence of concentration gradient is solved by Fick's first law as shown in an equation below.

$$J = -D\frac{dc}{dt}$$

Where J =   diffusion flux (mol m^{-2}s^{-1})

D =   diffusion coefficient (m^{2}s^{-1})

$\dfrac{dc}{dt}$ =   the rate of change of concentration in a certain area
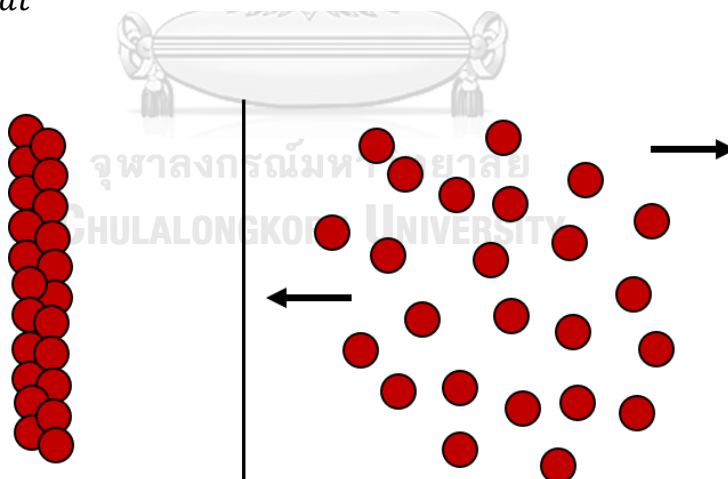
Figure 2.5 Mass transfer by diffusion transport. [34]

Migration is a movement of charged substance under the inducement of electrical field. This movement occurs when potential is applied to electrode surface in a solution containing ions that affects charge migration as shown in Figure 2.6. The donation of migration to the total flux is proportional to the charge of ion, the ion concentration, the electric field gradient and the diffusion coefficient.
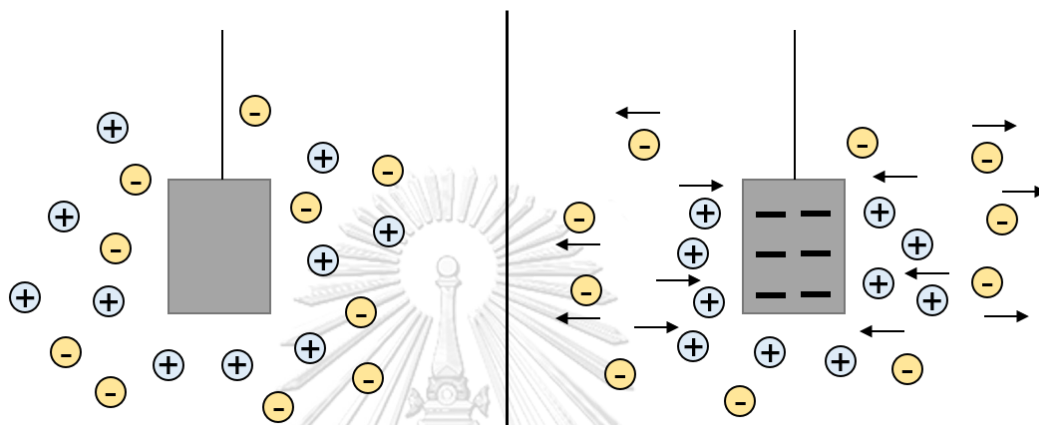
Figure 2.6 Migration mass transfer by applying negative charge at the electrode surface. [34]

Convection is a forced movement of the species by stirring in the system (hydrodynamics) as shown in Figure 2.7. The rate of stir solution can be controlled by the convective contribution to total flux of species which is described in hydrodynamic velocity.
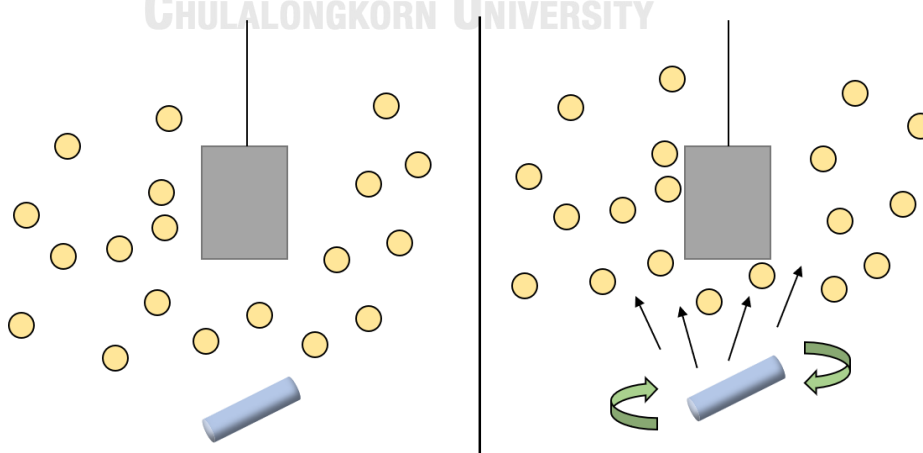
Figure 2.7 Convection mass transfer by stirring solution in the electrochemical system. [34]

2.1.4 Cyclic voltammetry (CV)

Cyclic voltammetry is a basic technique extensively used for the electrochemical characterization of the new electrode due to its simple use in case of preliminary study of the electroactive species in electrochemical reaction of the new system. For CV measurement, the potential is applied to the working electrode in two steps versus time as triangular waveform that is scanned forward and swept backward as shown in Figure 2.8.
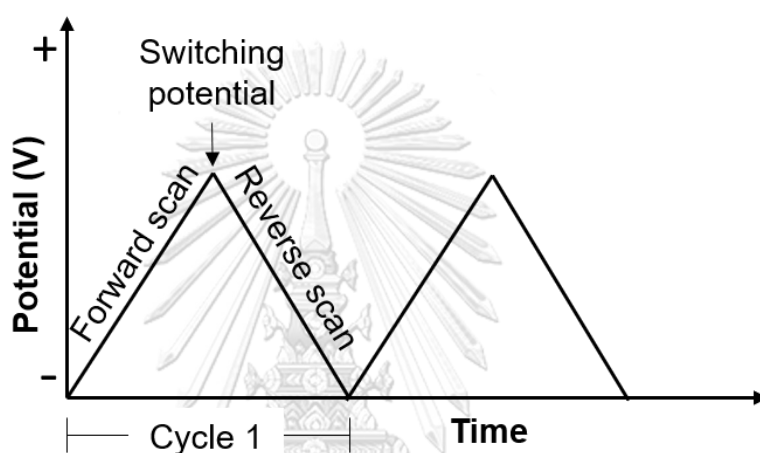
Figure 2.8 Cyclic potential waveform. [35]

When the potential is applied from positive to negative, important peak including an anodic peak and a cathodic peak occurs called cyclic voltammogram. At first half cycle, the cathodic peak occurs by reduction reaction which the height of this peak is called cathodic peak current (i_{pc}) and the potential at the highest peak is called cathodic peak potential (E_{pc}). For the backward cycle, the anodic peak occurs by oxidation reaction which the height of this peak is called anodic peak current (i_{pa}) and the potential at the highest peak is called anodic peak potential (E_{pa}). The graph plot between applied potential (v) and the current intensity (μA) is shown in Figure 2.9.
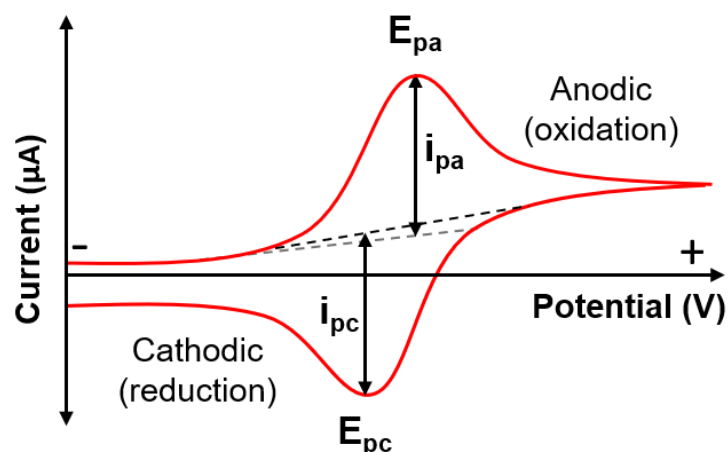
Figure 2.9 Cyclic voltammogram of reversible process [35]

2.1.4.1 Reversible system

The reversible system can be defined as a symmetrical peak shape of cathodic and anodic peak confirming that the electroactive species of target analytes can oxidize and reduce completely. This system has three characteristics to identify that the electrochemical behavior is reversible or non-reversible by the interpretation of the information obtained from cyclic voltammogram.

- The difference between E_{pc} and E_{pa} is close to $\dfrac{2.3\,RT}{nF}$ or $\dfrac{59}{n}$ at 25°C.

- The ratio of $\dfrac{i_{pa}}{i_{pc}}$ is equal to 1.

- The position of peak potential is independent from function of scan rate.

Normally, this system can be used for the determination of the number of transferred electrons and the peak current can be calculated by Randles-Sevcik equation as following.

$$i_p = (2.69 \times 10^5)n^{3/2}ACD_0^{1/2}v^{1/2}$$

Where	i_p	=	peak current
	n	=	number of transferred electrons
	A	=	area of electrode surface (cm^2)
	C	=	concentration of electoactive species (mol/cm^3)
	D_0	=	diffusion coefficient (cm^2/s)
	v	=	scan rate (V/s)

2.1.4.2 Quasi-reversible and irreversible system

The cathodic and anodic peak shapes of both systems are not symmetry because the reaction at the electrode surface is very slow to be measured the current signal. The voltammogram of irreversible system presents only cathodic peak current or anodic peak current as shown in Figure 2.10A. The voltammogram of quasi-reversible system as shown in Figure 2.10B displays an unequal peak height of cathodic and anodic currents with the increasing of scan rate. The current peak is calculated by equation below.

$$i_p = (2.99 \times 10^5)n\left(\propto n_a^{1/2}\right)AD_0^{1/2}Cv^{1/2}$$

Where $\propto$ is calculated from:

$$\left|E_p - E_{p/2}\right| = \frac{47.7}{\propto} \ (25°C)$$

Where $E_{p/2}$ is the potential of half peak current
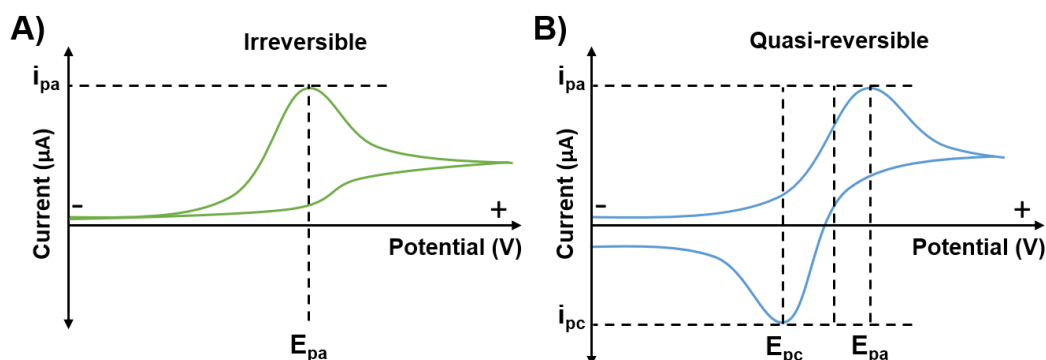
Figure 2.10 Cyclic voltammogram of (A) irreversible system and (B) quasi-reversible system. [36]

2.1.5 Differential pulse voltammetry (DPV)

DPV is a technique that a potential pulse is applied on a linear ramp potential. This technique uses for quantitative analysis and provides the sensitivity enhancement for low concentration analytes. Normally, cyclic voltammetry is used for preliminary study of the redox process of target analytes, however this technique is difficult to measure the faradaic currents due to the disturbed background current. To overcome this disadvantage, differential pulse voltammetry is more suitable for analysis because this technique can discriminate between faradaic current and charging current. The principle of this technique is to apply an amplitude potential in waveform as shown in Figure 2.11A. The current is immediately measured before and end the application of each pulse and the difference between them is recorded as shown in Figure 2.11B. The result of this technique is called differential pulse voltammogram and the analyte concentration is obtained from the height of peak current which is calculated by an equation.

$$i_{max} = \frac{nFAD_o^{1/2}C_0^*}{\pi^{1/2}(\tau - \tau')^{1/2}} \frac{(1 - \sigma)}{(1 + \sigma)}$$

Where $\sigma = exp\left[\frac{(nf)(\Delta E)}{(RT)(2)}\right]$, ($\Delta E$ is pulse amplitude) and maximum value of $\frac{(1-\sigma)}{(1+\sigma)}$ is equal to 1.
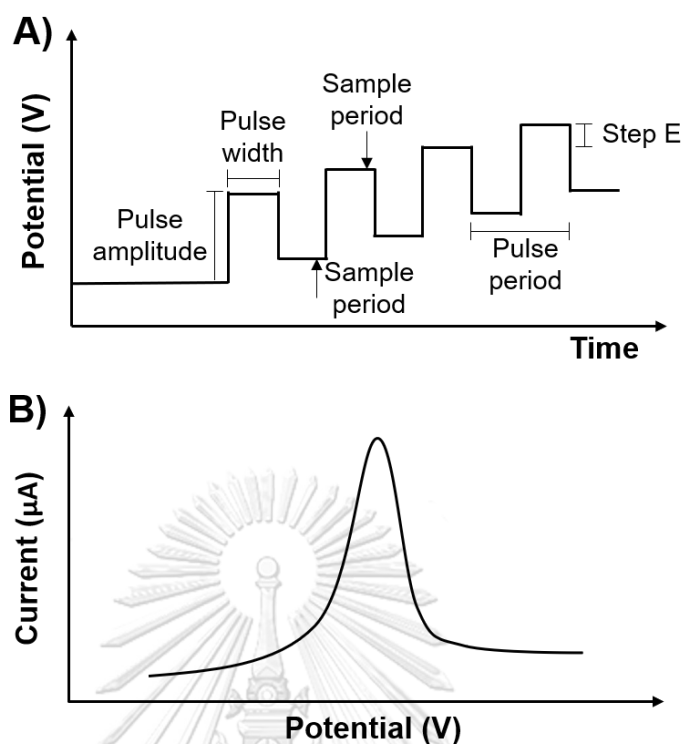
Figure 2.11 (A) Differential pulse potential waveform and (B) differential pulse voltammogram. [37]

2.1.6 Chronoamperometry

Chronoamperometry is an electrochemical technique which is very powerful for quantitative analysis. The result of peak current is obtained from two processes including the mass transfer which electroactive species are transferred from bulk solution to the electrode surface and the charge transfer that can occur the electron transfer in the working electrode surface. The result is recorded as a function of time at a constant potential and the response signal is plotted between current and time as shown in Figure 2.12. The current response of this method is correlated with the concentration of the oxidized or reduced species on the surface of working electrode which can be calculated by the Cottrell equation as following.

$$i_t = \frac{nFAC_oD_o^{1/2}}{\pi^{1/2}t^{1/2}}$$

Where i_t = the current at time t (s)

n = the number of electron (eq. mol^{-1})

F = Faraday's constant (96,485 C eq^{-1})

A = the geometric area of the electrode (cm^{-2})

C_o = the concentration of the oxidized species (mol cm^{-3})

D_o = the diffusion coefficient of the oxidized species (cm^2 s^{-1})
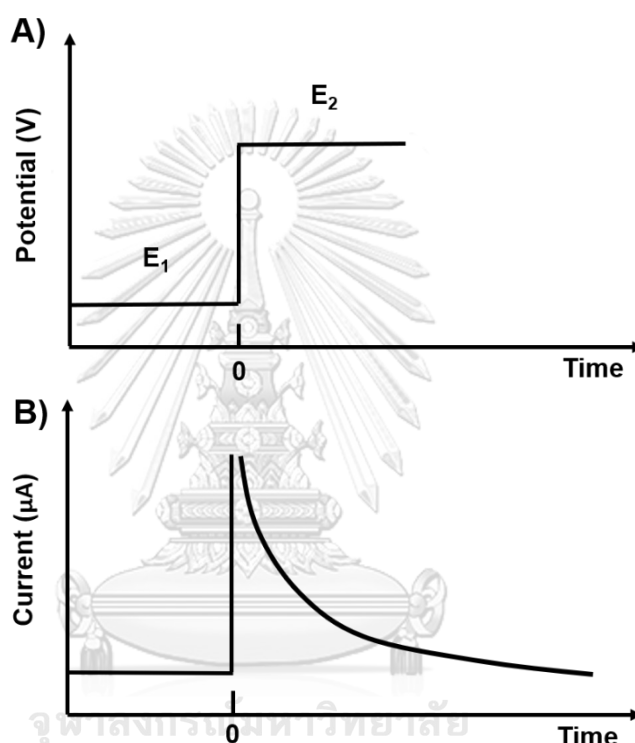
Figure 2.12 (A) Applied potential waveform in amperometric measurement and (B) amperogram of the electroactive species. [38]

2.1.7 Electrochemical impedance spectroscopy (EIS)

Electrochemical impedance spectroscopy (EIS) is an electrochemical technique for measuring the impedance of a system, which is depended of the alternating current (AC) potentials frequency. The concept of this method is to apply an AC to the electrical circuit of the system and measure as a function of frequency. The result is recorded as a function of the impedance and the frequency called Nyquist plot as shown in Figure 2.13. The impedance spectrum can be used to study the kinetic of electron transfer process and diffusion-limited process. The semicircle

diameter represents the charge transfer resistance (R_{ct}) of the measured electrochemical cell, and it can be calculated by the equation as shown in below.

$$R_{ct} = \frac{RT}{Fi_0}$$

Where R_{ct} =   electron transfer resistant

R =   gas constant

T =   temperature

F =   Faraday constant

i_0 =   the exchange current

Where i_0 is calculated from:

$$i_0 = FAk^0C$$

Where k^0 is rate constant and calculated from:

$$k^0 = \frac{RT}{R_{ct}FAC}$$
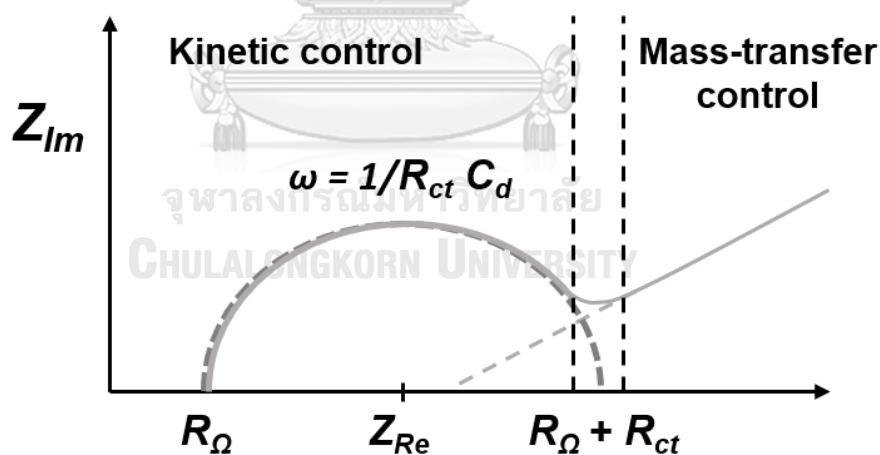
Figure 2.13 Electrochemical impedance spectrum in term of Nyquist plot. [39]

2.2 Electrode surface modification

The electrochemical system consists of three electrodes including working, reference and working electrodes. Among three electrodes, the working electrode is the most important one for analysis in the system because the electron transfer between the electroactive species of analytes and the working electrode surface is

focused. Currently, electrochemical sensor is fabricated into a small system for portability. Thus, the working electrode is designed in a small size and the surface area is limited leading to low electrochemical sensitivity of the system. To enhance sensitivity of the system, the nanomaterials are used for the modification on the working electrode surface because of their high specific surface area, high electrocatalytic activity, good electrical conductivity and good physical property. In this work, the carbon-based and metallic nanomaterials are investigated.

2.2.1 Nanomaterials

Nanomaterials are the chemical substances manufactured and used in a small scale. One dimension of nanomaterials is less than approximately 100 nanometers (nm). Due to their good chemical reactivity and high electrical property, nanomaterials are extensively used in various fields such as cosmetic, paint, textile, drug delivery, corrosion and electrochemical analysis.

2.2.1.1 Metallic nanoparticles

Metallic nanoparticles have recently become one of the most powerful materials in analytical chemistry due to their unique chemical, physical and electronic properties. These excellent properties can be used to construct novel sensor such as biosensor and electrochemical sensor. In general, metal nanoparticles have excellent conductivity and electrocatalytic properties which are suitable for enhancing the electron transfer between target analytes and working electrode surface and being catalysts to increase chemical reactions in the electrochemical system. Normally, the metallic nanoparticles including gold, silver, platinum, copper and palladium are employed to modify on electrode surface [40]. Among these metallic nanoparticles, gold nanoparticles (AuNPs), which possess high electron transfer, large surface area, high conductivity and high electrocatalytic properties, have been widely applied for both enzymatic and non- enzymatic sensors. Moreover, the gold nanoparticles have a good biocompatibility which can be immobilized on biomolecules without bioactivity loss [41, 42]. The morphology of gold nanoparticles is shown in Figure 2.18.
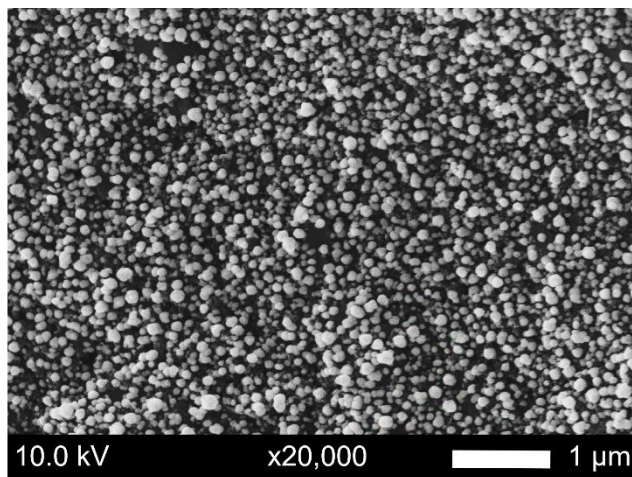
Figure 2.14 SEM image of gold nanoparticles.

Khater, M. *et.al.* [43] designed a label-free biosensor for the detection of *citrus tristezza virus* (CTV). The sensor platform was modified on a screen-printed carbon electrode (SPCE) with AuNPs followed by immobilizing with thiolated ssDNA probes to enhance the electrode conductivity. This sensor showed high selectivity toward CTV detection with the linear range of 0.1 to 10 μM. Moreover, the developed sensor demonstrated the good performance in a real plant sample matrix.

He, B. *et.al.* [44] developed AuNPs and graphene nanocomposite modified on a thin film gold electrode for the detection of nitrofurazone and semicarbazide. This modified sensor can enhance electron transfer and the results showed high sensitivity toward NF and SC detections with the linear responses and limits of detection of 0.2 to 4800 μM and 0.13 μM for NF, 0.02 to 2000 μM and 0.0047 μM for SC, respectively. This sensor was successfully applied for the determination of semicarbazide in real samples.

Hassani, S. *et.al.* [45] developed a highly sensitive label-free electrochemical aptasensor for the detection of diazinon. This sensor was assembled using a screen-printed electrode modified by gold nanoparticles. This sensor showed good sensitivity for diazinon detection with the linear range of 0.1 to 1000 nM and lower limit of detection of 0.0169 nM compared to other techniques including HPLC and colorimetric. Moreover, this aptasensor exhibited easy to use and low cost with good stability and reproducibility.

Bernardo-Boongaling, V.R.R. *et.al.* [46] synthesized gold nanoparticles modified on screen-printed electrode for the electrochemical determination of the aminothiols cysteine (Cys), methionine (Met), glutathione (GSH) and homocysteine (hCys). This modified sensor can enhance electron transfer between Cys, Met, GSH and hCys on the surface electrode. The modified electrode showed high performance of sensitivity, reproducibility, repeatability, linear range and limit of detection compared to the unmodified electrode. Moreover, device was successfully applied for the determination of cysteine and methionine in real dietary supplement samples.

2.3 Non- invasive sensor

Non-invasive chemical sensor can be defined as a medical procedure without breaking in skin and contacting with mucosa. The sensor is designed to measure body fluids without the use of needle leading to the detection of analytes without painfulness. The non-invasive chemical sensor can measure the metabolites, electrolytes (*e.g.* heavy metal ions, calcium, sodium, chlorine, potassium), glucose, urea, lactate, uric acid associated with body biofluids (*e.g.* saliva, tears, urine). Recently, there are reports that the non-invasive sensor coupled with electrochemical techniques can be used to detect target analytes in metabolites of body which exhibits high performance, rapid response, inherent miniaturization and low cost [47, 48].

Aparna, T. *et.al.* [49] fabricated gold-copper oxide/ reduced graphene oxide nanocomposite (Au-Cu$_2$O/rGO) based on electrochemical sensor for non-invasive determination of dopamine (DA) and uric acid (UA). This sensor can enhance electron catalytic activity for DA and UA detection. This non-invasive based electrochemical sensor showed high sensitivity, selectivity and simultaneous detection of DA and UA with the detection limit of 3.9 μM for DA and 6.5 μM for UA, respectively. Moreover, this sensor showed long-term stability and reproducibility and successfully applied for the quantification of DA and UA in urine samples.

Xuan, X. *et.al.* [50] fabricated reduced graphene oxide nanocomposite (rGO) based on electrochemical sensor for non-invasive detection of glucose. This sensor

exhibited excellent amperometric response to glucose with a linear range of 0─2.4 mM and a detection limit of 5.0 µM. This non-invasive electrochemical sensor showed high performance of sensitivity and stability for low glucose concentration. Moreover, this sensor can be applied for the quantification of glucose in sweat sample.

Recently, the substrates used for a non-invasive sensor have been developed in different platforms, such as tattoo [51, 52], paper [53], stretchable elastomer [54] and thread textile [55]. Among all, the thread textile has become the most attractive material used for the non-invasive sensor fabrication owing to its advantages, such as flexibility, durability, biocompatibility, breathability, high-water absorption and low cost.

Gaines, M. *et.al.* [56] fabricated electrochemical sensor for the detection of glucose using nylon thread-based electrodes. Glucose oxidase enzyme was employed to enhance sensitivity and selectivity of the system. The results showed high specificity and good linearity from 0 to 25 mM for glucose detection. Moreover, this thread-based electrode system was a viable sensor platform for detecting glucose in the physiological range.

Liu, X. *et.al.* [55] fabricated thread-based electrochemical sensors on gauze for rapid determination of uric acid (UA) as shown in Figure 2.19. This sensor used enzyme to enhance sensitivity and selectivity of the system. The results showed high specificity and good linearity from 0 to 800 µM, and excellent reproducibility for UA detection. This sensor evaluated the robustness of thread-based biosensor due to its ability of accurate measurements for up to 7 h and excellent resilience against mechanical strain and deformation. Moreover, this sensor can be directly applied as wearable sensor for monitoring of UA on wound.

Figure 2.15 The wearable electrochemical sensors on gauze [55]

2.4 Uric acid (UA)

Uric acid (UA) is chemically designated as 2,6,8-tryhydroxypurine which is the final product of purine metabolism. The normal levels of UA are between 0.13 and 0.46 mM in serum and 1.4 and 4.46 mM in urine [57]. UA is an important biomarker in serum, urine, and other body fluids because the abnormal levels of UA can indicate various diseases such as gout, hyperuricemia, leukemia and Lesh-Nyhan syndrome [58]. Therefore, the detection of UA is crucial for disease diagnosis. Various methods have been reported for the determination of UA such as colorimetric method, enzymatic method, chemiluminescence method, fluorescence method, and electrochemical method. However, the limitations are high cost, requirement of additional step, specialist and complicated instrumental analysis. Therefore, this work focuses on electrochemical method as a non-invasive electrochemical sensor for UA determination due to its specificity, high sensitivity, rapidity, easy miniaturization, simple operation and low cost.

Liu, L. *et.al.* [59] synthesized nitrogen cobalt-doped porous carbon (CNCo) modified on glassy carbon electrode for the electrochemical determination of UA. This modified sensor enhanced electrochemical catalytic activity toward UA and provided good reproducibility and repeatability with a linear range of 2.0—110 μM and low detection limits of 0.83 μM. Moreover, the modified sensor was successfully employed to quantify UA in real samples with high recoveries.

Sha, R. *et.al.* [60] fabricated molybdenum disulfide (MoS_2) on an aluminium foil (Al) as electrochemical sensor for the detection of UA. This sensor showed excellent sensitivity, reproducibility and selectivity towards UA with a linear range of 10—400 µM and low detection limit of 1.169 µM. Moreover, the sensor was also successfully evaluated for the detection of UA in human urine sample compared to the conventional biochemical tests in clinical laboratory.

Reddy, Y.V.M. *et.al.* [61] synthesized silicon dioxide/iron oxide nanocomposited (SiO_2/Fe_3O_4) modified on carbon paste electrode (CPE) as UA sensor. This electrochemical sensor showed an excellent electrochemical activity towards the detection of UA. The analytical performance of this sensor exhibited a good limit of detection of 0.4 µM with a linear range of 1.2—8.2 µM and showed a stable response even in the presence of interferences (ascorbic acid and dopamine). Moreover, this developed sensor was also successfully applied for the determination of UA in real sample.

CHAPTER III

EXPERIMENTAL

For this chapter, the information of chemical and reagent, instrument, preparation procedure, electrochemical detection and real sample analysis are given as following.

3.1 Chemical and reagent

- Carbon ink (Gwent group, Torfaen, United Kingdom).
- Chloroauric acid tetrahydrate ($HAuCl_4$) (Sigma–Aldrich, St. Louis, MO, USA).
- Disodium hydrogen phosphate (Na_2HPO_4) (Carlo Erba Reagenti-SDS, Val de Reuil, France).
- Potassium chloride (KCl) (Carlo Erba Reagenti-SDS, Val de Reuil, France).
- Potassium dihydrogen phosphate (KH_2PO_4) (Carlo Erba Reagenti-SDS, Val de Reuil, France).
- Potassium ferricyanide ($K_3[Fe(CN_6)]$) (Sigma–Aldrich, St. Louis, MO, USA).
- Potassium ferrocyanide ($K_4[Fe(CN_6)]$) (Sigma–Aldrich, St. Louis, MO, USA).
- Silver/silver chloride ink (Ag/AgCl) (Gwent group, Torfaen, United Kingdom).
- Sodium chloride (NaCl) (Carlo Erba Reagenti-SDS, Val de Reuil, France).
- Sodium hydroxide (NaOH) (Merck, Schuchardt OHG 85662 Hohenbrunn Germany).
- Sulphuric acid (H_2SO_4) (Carlo Erba Reagenti-SDS, Val de Reuil, France).
- Uric acid (UA) (Sigma–Aldrich, St. Louis, MO, USA).

3.2 Instrument

- Potentiostat CHI1240B (CH Instruments, Inc., Austin, TX, USA)
- Scanning electron microscopy (SEM) with energy dispersive X-rays spectroscopy (EDX) (JSM-6400; Japan Electron Optics Laboratory Co., Ltd., Tokyo, Japan)
- Screen frame (Chaiyaboon Co., Bangkok, Thailand)

3.3 Preparation of the stock solutions for electrochemical detection of uric acid

3.3.1 Preparation of 0.5 M potassium chloride

1.86 g of potassium chloride was dissolved in 50 mL of Milli-Q water.

3.3.2 Preparation of 5.0 mM ferri/ferrocyanide

105.6 mg of potassium ferricyanide and 82.3 mg of potassium ferrocyanide were dissolved in 50 mL of 0.5 M potassium chloride.

3.3.3 Preparation of 0.1 M phosphate buffer saline solution (PBS)

0.71 g of potassium dihydrogen phosphate (KH_2PO_4), 0.68 g of disodium hydrogen phosphate (Na_2HPO_4), 0.29 g of sodium chloride (NaCl) and 0.37 g of potassium chloride (KCl) were dissolved in 50 mL of Milli-Q water.

3.3.4 Preparation of 1.0 M sodium hydroxide

1.0 g of sodium hydroxide was dissolved in 25 mL of Milli-Q water.

3.3.5 Preparation of 1.0 mM uric acid

1.7 mg of uric acid was dissolved in 100 µL of 1.0 mM sodium hydroxide and 10 mL of 0.1 M PBS.

3.4 Carbon-coated cotton thread preparation

3.4.1 Preparation of carbon ink

1.0 g of carbon ink was dissolved in 600 µL of butyl glycol acetate and methylene glycol monobutyl.

3.4.2 Preparation of carbon-coated cotton thread

A carbon-coated cotton thread as working electrode (WE) was fabricated by coating cotton thread with the prepared ink as following method. Briefly, the cotton thread (DMC mouline special 25 100% cotton B5200) was soaked in the prepared carbon ink and passed through a pinhole of a needle tip followed by baking at 55 °C for 30 min in the oven as shown in Figure 3.1. The carbon-coated cotton thread was obtained and used as the WE for all further experiments.
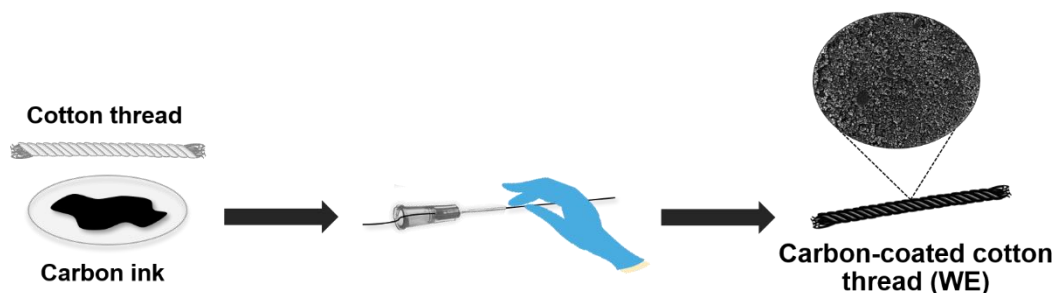
Figure 3.1 Schematic of conductive cotton thread preparation for fabricating WE.

3.5 The device design

3.5.1 Fabrication of screen-printed electrode (SPE)

The pattern of SPE was designed by Adobe Illustrator consisting of counter and reference electrodes as shown in Figure 3.2. Both electrodes were fabricated through an in-house screen-printing technique. First, the carbon ink was screened on polyvinylchloride (PVC) substrate as a counter electrode (CE) and baked at 55 °C for 30 min in an oven. After that, the Ag/AgCl ink was screened on the same PVC substrate as a reference electrode (RE) and dried at 55 °C for 1 h in an oven. The width and length of CE and RE are 0.95 mm and 25 mm, respectively.
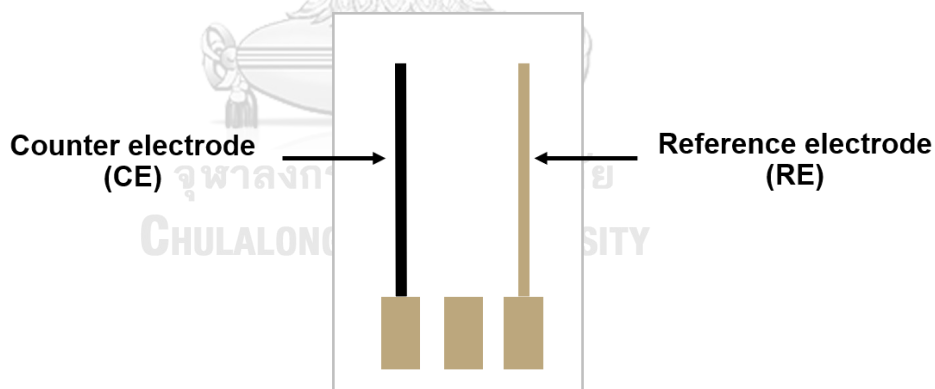
Figure 3.2 Configuration of the SPE.

3.5.2 Fabrication of cotton thread-based sensor

After obtaining the SPE, a cotton thread-based sensor was fabricated consisting of RE, WE and CE as shown in Figure 3.3. Initially, a transparency film was punched in a hole diameter of 6 mm and attached on the prepared SPE using double-side tape for creation of electrochemical test zone and hydrophobic barrier. After that, the

carbon-coated cotton thread was placed and attached between the RE and CE, and a cotton thread-based sensor was obtained and kept for further modification.

RE: Ag/AgCl SPE on PVC, **WE**: carbon-coated cotton thread, **CE**: Carbon SPE on PVC
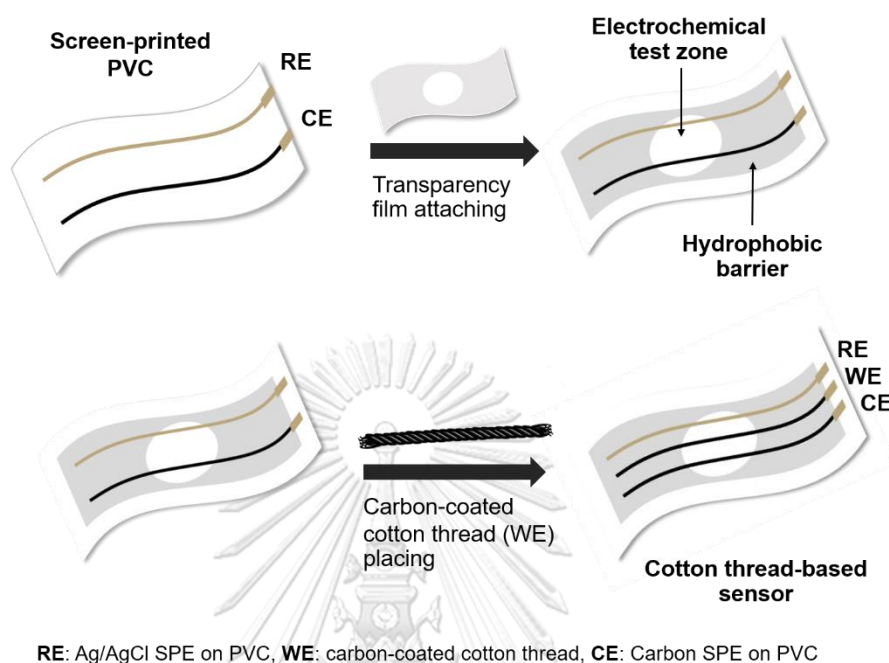
Figure 3.3 Schematic of cotton thread-based electrochemical sensor preparation.

3.6 Modification of cotton thread-based sensor

3.6.1 Preparation of stock solution for electrode modification

3.6.1.1 Preparation of 0.1 M sulphuric acid

139.1 µL of 17.97 M sulphuric acid was dissolved in 25 mL of Milli-Q water.

3.6.1.2 Preparation of 3.0 mM chloroauric acid tetrahydrate

3.0 mM of chloroauric acid was prepared by adding 11.8 mg of chloroauric acid in 10 mL of 0.1 M sulphuric acid.

3.6.2 Electrochemical deposition of gold nanoparticles on cotton thread-based sensor

To modified gold nanoparticles (AuNPs) on the WE, 40 µL of 3.0 mM HAuCl$_4$ was dropped on the electrochemical test zone of the sensor followed by applying a deposition potential of -0.6 V (vs. Ag/AgCl) for 120 s [62]. The AuNPs were obtained on the surface of carbon-coated cotton thread (WE). After modification, AuNPs modified cotton thread-based sensor was carefully rinsed with Milli-Q water and dried in the oven at 55 °C for 1 h prior to use.

3.7 Optimization of cotton thread-based sensor modification

Two main factors for the cotton thread-based sensor modification (*e.g.* $HAuCl_4$ concentration and electrodeposition time of AuNPs) were optimized to obtain the highest current response for uric acid detection. The optimization was investigated using differential pulse voltammetry (DPV), and the potential was scanned from -0.3 V to +0.8 V for 1.0 mM uric acid.

3.7.1 Effect of $HAuCl_4$ concentration

The different concentrations of $HAuCl_4$ concentration were investigated at 1.0, 2.0, 3.0, 4.0 and 5.0 mM in electrodeposition of AuNPs on the cotton thread-based sensor.

3.7.2 Effect of electrodeposition time of AuNPs

The effect of electrodeposition time was investigated using by varying of the AuNPs electrodeposition time on cotton thread-based sensor including 30, 60, 120, 180 and 240 s.

3.8 Optimization of parameters in differential pulse voltammetric measurement (DPV parameters)

The optimization of DPV parameters was investigated by measuring the DPV response of 25 µM of uric acid. The step potential in the range of 3—20 mV, the amplitude in the range of 50—250 mV and the pulse width in the range of 30—150 ms were studied.

3.9 Characterization of the modified cotton thread-based sensor

3.9.1 Surface morphology characterization

The surface morphologies of unmodified and modified cotton thread-based sensors were characterized using scanning electron microscopy (SEM) with energy dispersive X-rays spectroscopy (EDX).

3.9.2 Electrochemical characterization

The electrochemical measurements were performed using potentiostat CHI1240B via cyclic voltammetry (CV) and differential pulse voltammetry (DPV). The modified cotton thread-based sensor was electrochemically characterized by CV using a standard solution of 5.0 mM $[Fe(CN)_6]^{3-}/^{4-}$ with the potential range from -0.9 V to +1.2

V and a scan rate of 100 mV/s. Furthermore, the sensor was also characterized via DPV using 1.0 mM uric acid with the potential range from -0.3 V to +0.8 V.

3.10 The analytical performances of AuNPs modified cotton thread-based sensor

The investigation of analytical performances was performed on DPV measurement.

3.10.1 Calibration curve

5.0 mM uric acid stock solution was diluted to different concentrations from 10 µM to 5 mM and then employed for DPV measurement using AuNPs modified cotton thread-based sensor. After that, a linear relationship between concentration of uric acid and anodic current response was plotted to obtain a linear range of the system.

3.10.2 Limit of detection (LOD)

The limit of detection (LOD) was calculated via the equation of LOD=3S/N, where S is a standard deviation of a signal obtained from a blank solution (seven-time determinations) and N is a slope of calibration curve.

3.10.3 Interferent study

The stock solution of potential interferences (10.0 mM) including KCl, NaCl, glucose, creatinine, urea, 1.0 mM stock solution of ascoric acid and 1% excess of BSA were prepared. The selectivity of modified cotton thread-based sensor was evaluated by measuring of 1.0 mM uric acid in the presence of different interferences. In this study, the tolerance limit is defined as the molar ratio of potential interferences/uric acid that caused the ±5% change in the current response of uric acid.

3.10.4 Stability of the sensor

The storage stability of the AuNPs modified cotton thread-based sensor was studied by keeping the sensor at the room temperature in desiccator for 30 days. The measurement of DPV response to 1.0 mM of UA in PBS solution multiple times was used to investigate the stability of the sensor.

3.10.5 Real sample analysis

3.10.5.1 Real sample preparation

The standard calibration curve with spiking method was selected for the detection of UA in pooled urine sample. The pooled urine sample was collected from 5 different healthy adults to verify the variety of samples with non-bias prior to medical diagnosis application. The sample was diluted with 0.1 M of PBS solution (pH 6) in a ratio of 1:1. Next, the known amounts of UA (0.5, 1.0 and 2.0 mM) were added to the diluted samples and then 40 μL of sample was finally analyzed on the modified cotton thread-based sensor via DPV.

3.10.5.2 Recovery percentage

The percentage of recovery for real sample analysis was employed to evaluate the applicability of the purposed sensor using standard addition method. The percentage of recovery was calculated from the equation below.

$$\% \, Recovery = \frac{Measured \, value \, of \, spiked \, sample - Measured \, value \, of \, unspiked \, sample}{Known \, value \, of \, spiked \, sample} \times 100$$

3.10.5.3 Laser desorption ionization mass spectroscopy (LDI-MS)

For method validation, LDI-MS was employed to validate the applicability of the proposed sensor. This technique is a soft ionization technique that has been widely applied in various fields of applications, such as proteomic, genomic, biomedical and forensic studies. LDI-MS is an analytical technique using pulse laser as an energy source for ionization and fragmentation of molecule. The laser is generally a UV laser, which commonly includes a nitrogen laser (λ=337 nm) or Nd-YAG laser (λ=355 nm).

CHAPTER IV

RESULTS AND DISCUSSION

For this chapter, the results including physical characterization, electrochemical characterization, optimization of cotton thread-based sensor, optimization of parameter for uric acid detection and the analytical performances of the cotton thread-based sensor were systematically investigated and discussed.

4.1 Physical characterization of cotton thread-based sensor

After fabrication of the cotton thread-based working electrode (WE), the prepared WE was characterized by scanning electron microscopy (SEM) with energy dispersive X-rays spectroscopy (EDX) to investigate the surface morphologies (Figure 4.1). As shown in Figure 4.1A, a SEM image displayed that the morphology of the uncoated cotton thread was quite smooth, whereas the carbon-coated cotton thread showed higher surface roughness than the uncoated one (Figure 4.1B). To further enhance the specific surface area and electrochemical conductivity of the cotton thread-based sensor, gold nanoparticles (AuNPs) were modified on the surface of the carbon-coated cotton thread through electrodeposition. The AuNPs were uniformly decorated on the surface of carbon-coated cotton thread (Figure 4.1C) with an average particles size of 98.10 ± 10.42 nm (n=20). Moreover, the result obtained from EDX clearly identified the characteristic peaks of Au as shown in Figure 4.2. The weight contents of C, O and Au were 74.59%, 1.59% and 23.82%, respectively, and the atom contents of C, O and Au were 96.57%, 1.55% and 1.88%, respectively. Therefore, these results confirmed that the AuNPs were successfully electrodeposited on the carbon-coated cotton thread and ready to be used as the modified cotton thread-based sensor.
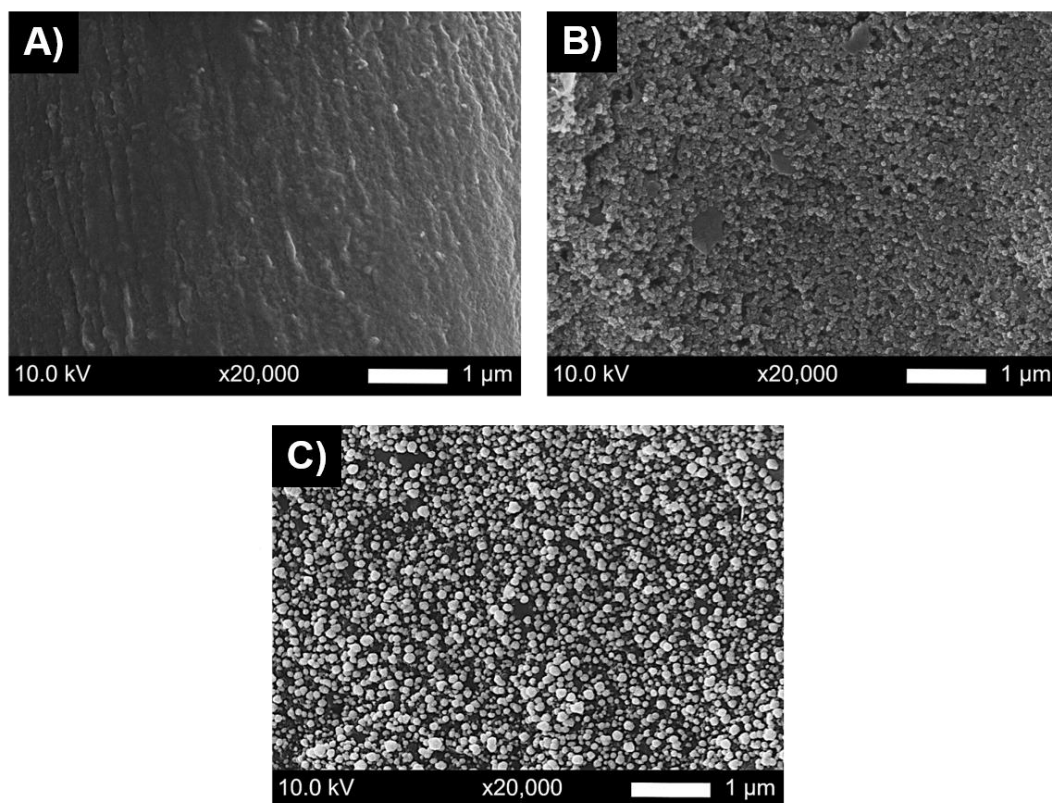
Figure 4.1 SEM images of (A) uncoated cotton thread, (B) carbon-coated cotton thread and (C) AuNPs modified carbon-coated cotton thread with a magnification of 20,000**x.**
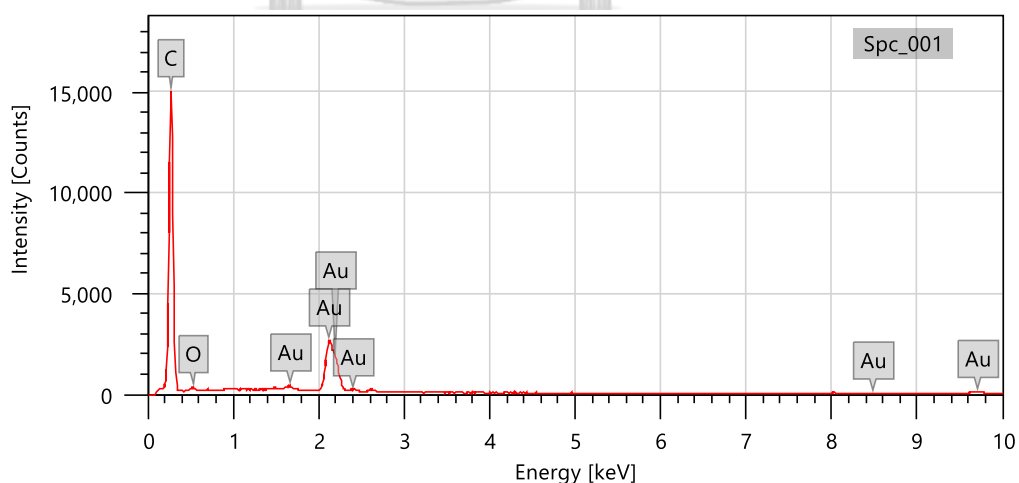
Figure 4.2 SEM-EDX spectrum of AuNPs modified carbon-coated cotton thread.

4.2 Electrochemical characterization of the modified cotton thread-based sensor

To characterize the electrochemical properties of the modified cotton thread-based sensor, the electrochemical behaviors of the carbon-coated cotton thread in the presence and absence of AuNPs were investigated by using cyclic voltammetry (CV) in the presence of 5.0 mM $[Fe(CN)_6]^{3-/4-}$ in 0.1 M KCl as shown in Figure 4.3A and B. From the cyclic voltammograms, the presence of AuNPs on the carbon-coated cotton thread (green line) showed higher anodic and cathodic peak currents towards $[Fe(CN)_6]^{3-/4-}$ detection, which was approximately 2 times higher than the one without AuNPs (pink line). The incorporation of AuNPs on the surface of the carbon-coated cotton thread can improve both electrochemical conductivity and specific surface area of the cotton thread-based sensor, leading to enhanced electrochemical performances of the sensor.
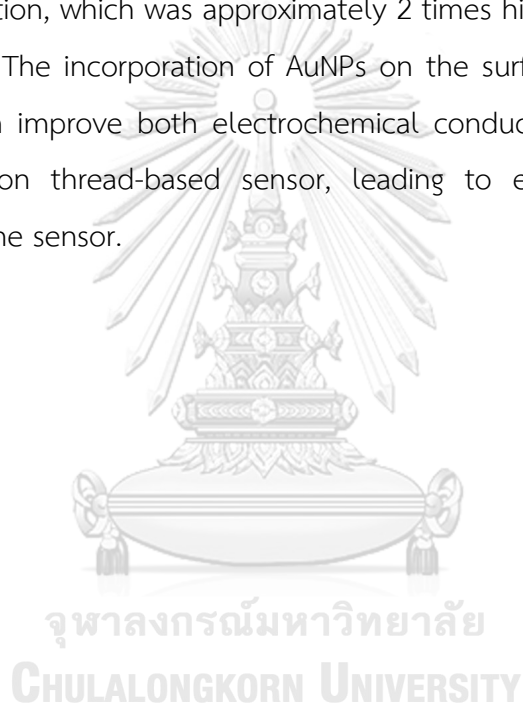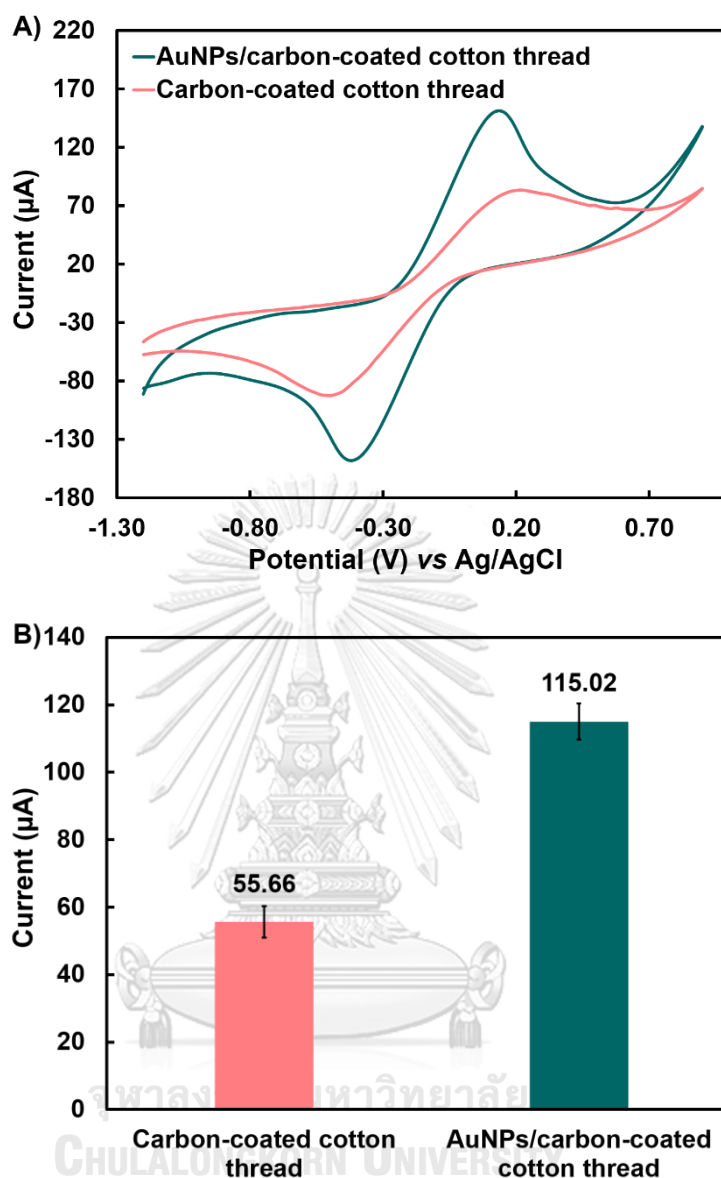
Figure 4.3 (A) Cyclic voltammograms of 5.0 mM $[Fe(CN)_6]^{3-/4-}$ measured on the AuNPs/carbon-coated cotton thread and carbon-coated cotton thread with a scan rate of 100 mV/s and (B) the anodic peak currents obtained from cyclic voltammograms in Figure 4.3A.

To evaluate the analytical performance of the modified cotton thread-based sensor, 1.0 mM UA was measured using differential pulse voltammetry (DPV) as shown in Figure 4.4A and B. The anodic peak current response of UA measured on the AuNPs/carbon-coated cotton thread (yellow line) significantly increased compared with the one measured on the unmodified carbon-coated cotton thread

(blue line). These results indicated that the decoration of AuNPs on the cotton thread-based sensor can substantially enhance the electrochemical activity toward UA detection due to the high electrochemical active site of AuNPs for sensitive signal responses.
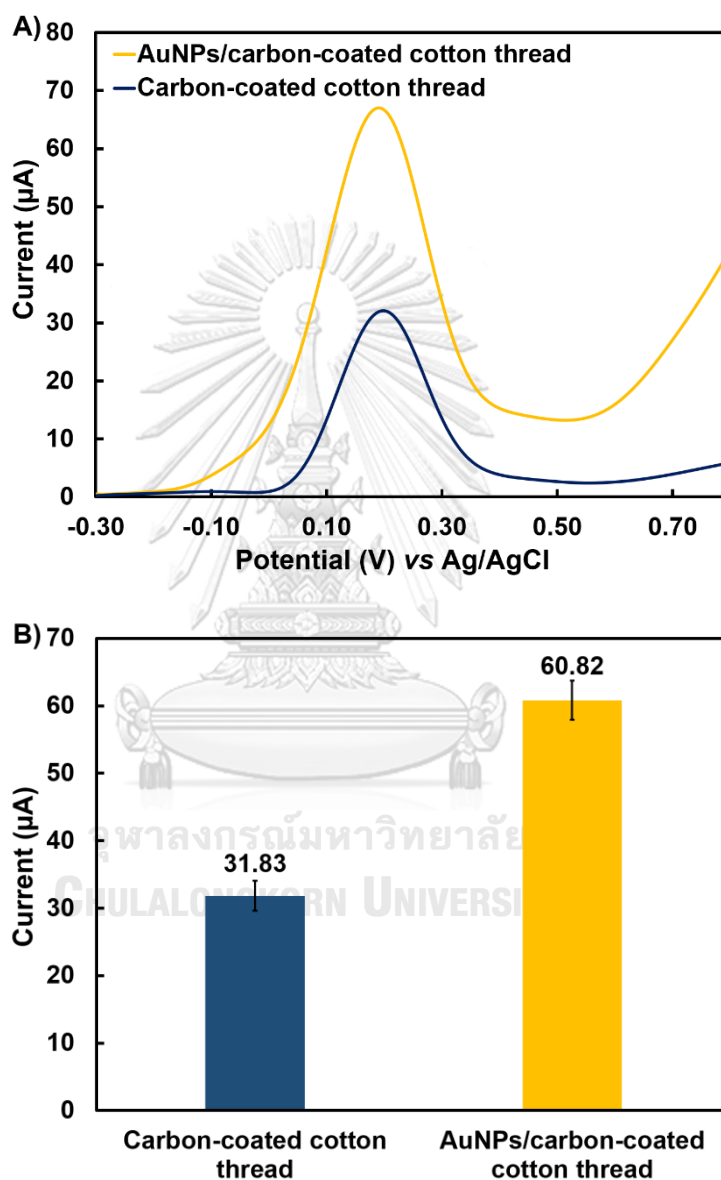
Figure 4.4 (A) Differential pulse voltammograms of 1.0 mM UA on AuNPs/carbon-coated cotton thread and carbon-coated cotton thread and (B) anodic peak currents obtained from differential pulse voltammograms in Figure 4.4A.

Moreover, electrochemical impedance spectroscopy (EIS) was also used to confirm the sensitivity of AuNPs modified cotton thread-based electrode by

measuring the change of impedance. As shown in Figure 4.5, the smallest semicircle was observed for the AuNPs modified cotton thread-based sensor. The low charge transfer resistance occurred because the AuNPs modified sensor (blue) can effectively accelerate the charge transfer through the sensor surface. For EIS spectrum of the unmodified cotton thread-based sensor (orange), the higher R_{ct} value was observed indicating a higher charge transfer resistance. Therefore, AuNPs modified cotton thread-based sensor was suitable to use as a sensitive sensor for UA detection.
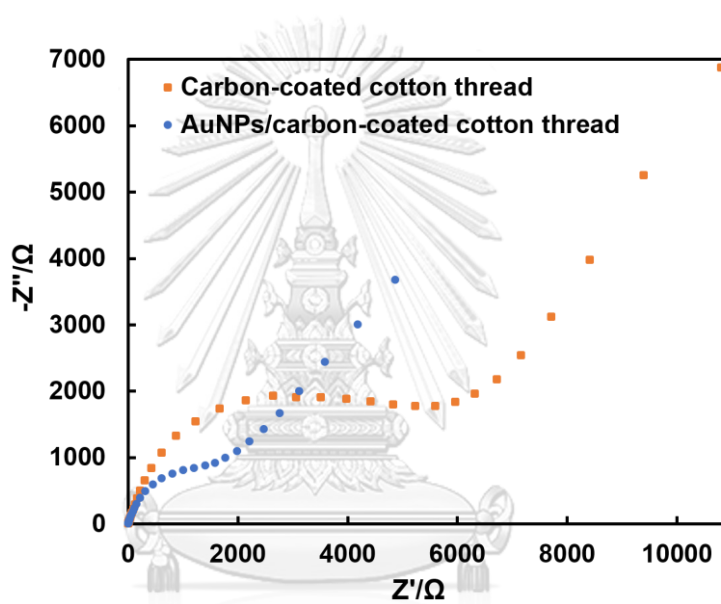
Figure 4.5 Nyquist plots of 2.0 mM $[Fe(CN)_6]^{3-/4-}$ on the AuNPs/carbon-coated cotton thread and carbon-coated cotton thread.

4.3 Optimization of the cotton thread-based sensor

For the cotton thread-based sensor fabrication, two-step fabrication including soaking and electrodeposition was used to create the AuNPs/carbon-coated cotton thread. Initially, the cotton threads were soaked in carbon ink and passed through the pinhole to create the uniform coating. Then, $HAuCl_4$ were electrodeposited to form AuNPs onto the carbon-coated cotton thread. For the modification of the sensor, various parameters affecting the electrochemical performances of the sensor were systematically optimized such as the concentration of $HAuCl_4$ and electrodeposition time of AuNPs.

4.3.1 An effect of HAuCl$_4$ concentration

An effect of HAuCl$_4$ concentration was varied in a range from 1.0 to 5.0 mM. As shown in Figure 4.6A and B, five different concentrations of HAuCl$_4$ were electrodeposited on the surface of the sensor at the deposition potential of -0.6 V for 120 s. The results showed that the anodic peak current response increased with the increasing of the concentration of HAuCl$_4$, and the highest anodic peak current was obtained at 3.0 mM of HAuCl$_4$. After that, the anodic peak current responses decreased at the concentrations more than 3.0 mM due to the higher density of gold cluster that can cause the agglomeration in some regions (Figure 4.7) leading to decreased surface area and electrochemical response of the system. Thus, the concentration of HAuCl$_4$ at 3.0 mM providing the well dispersion was selected as an optimal concentration for the sensor modification.
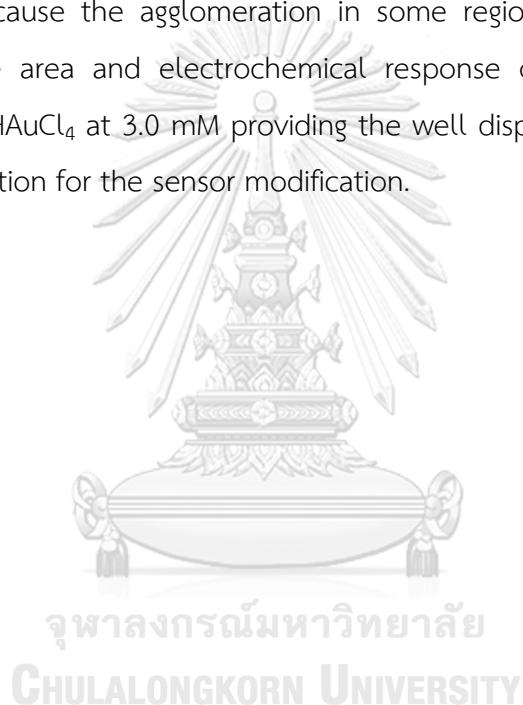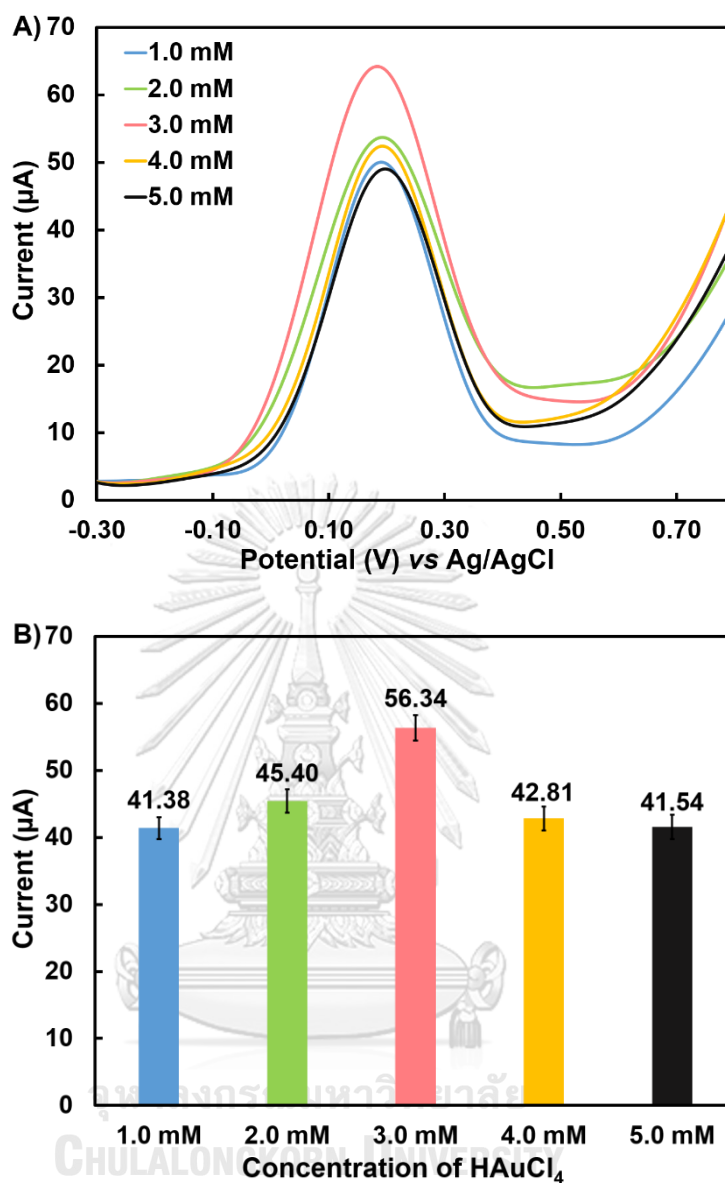
Figure 4.6 (A) Differential pulse voltammograms of 1.0 mM uric acid using AuNPs/carbon-coated cotton thread with different concentrations of $HAuCl_4$ (1.0, 2.0, 3.0, 4.0 mM and 5.0 mM) for AuNPs decorated on the cotton thread-based sensor and (B) anodic peak currents obtained from differential pulse voltammograms in Figure 4.6A.
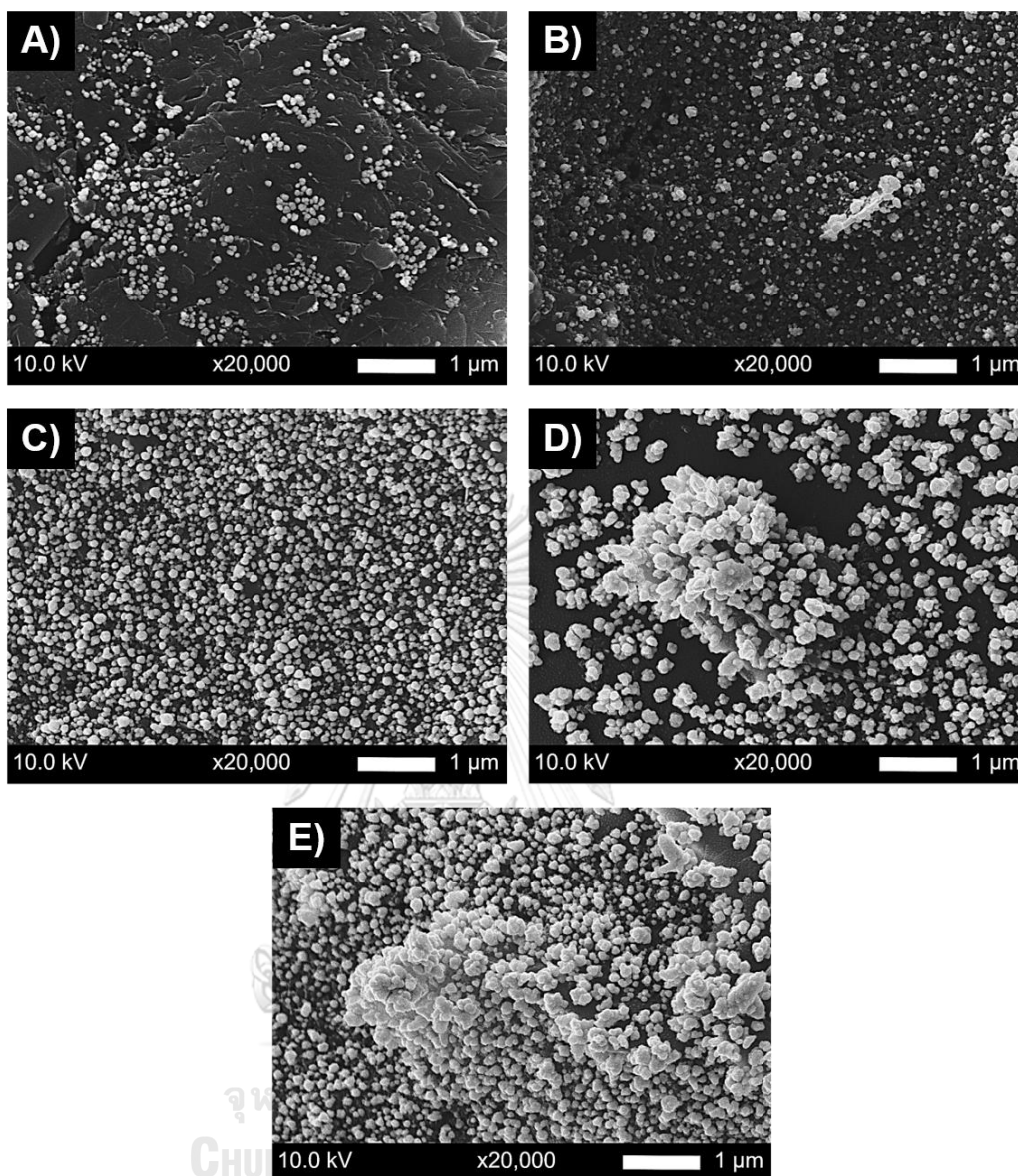
Figure 4.7 SEM images of the AuNPs/carbon-coated cotton thread with different concentrations of HAuCl$_4$, (A) 1.0 mM, (B) 2.0 mM, (C) 3.0 mM, (D) 4.0 mM and (E) 5.0 mM with a magnification of 20,000×.

4.3.2 An effect of electrodeposition time

An effect of electrodeposition time of AuNPs on the sensor was also investigated in a range of 30-240 s. As shown in Figure 4.8A and B, the anodic peak current increased when the electrodeposition time increased and the highest anodic peak current was obtained at 120 s of deposition time. Then, the anodic peak current response decreased with the increasing of the electrodeposition time more than 120

s because of the formation of the denser gold cluster aggregated in some regions (Figure 4.9) leading to decreased surface area and electrochemical responses. Thus, 120 s of electrodeposition time was chosen for the further experiments.
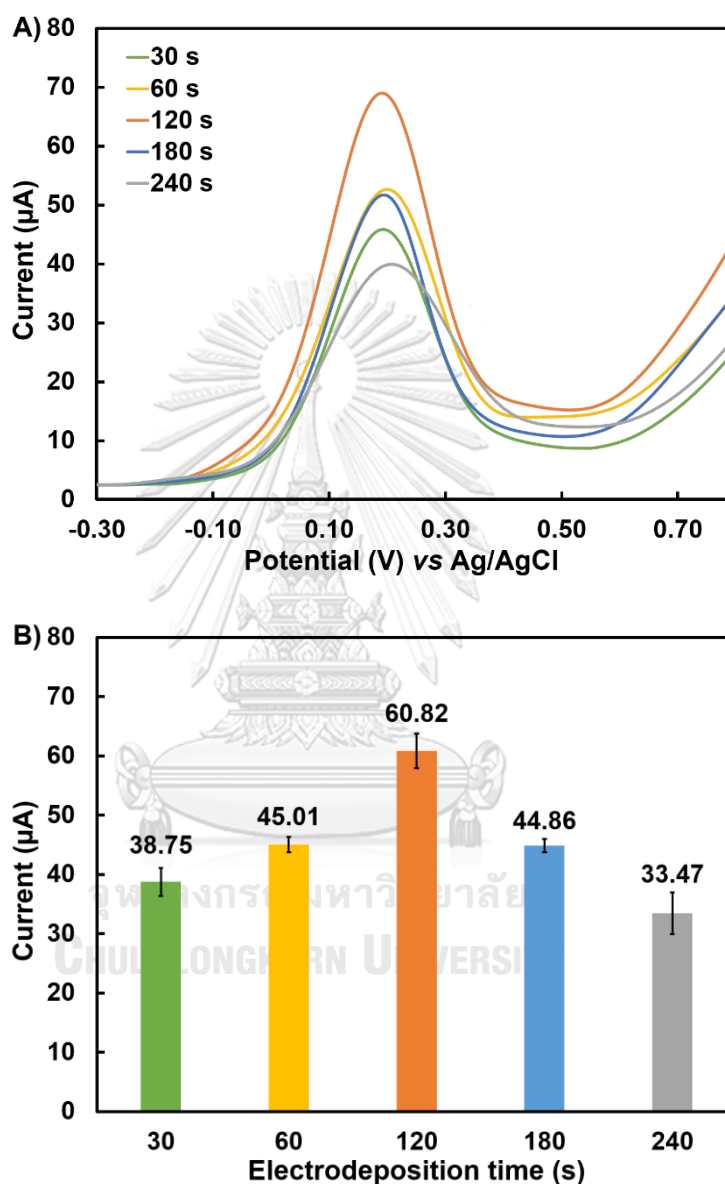
Figure 4.8 (A) Differential pulse voltammograms of 1.0 mM uric acid using the AuNPs/carbon-coated cotton thread with different electrodeposition times (30, 60, 120, 180 and 240 s) for AuNPs decorated on the cotton thread-based sensor and (B) anodic peak currents obtained from differential pulse voltammograms in Figure 4.8A.
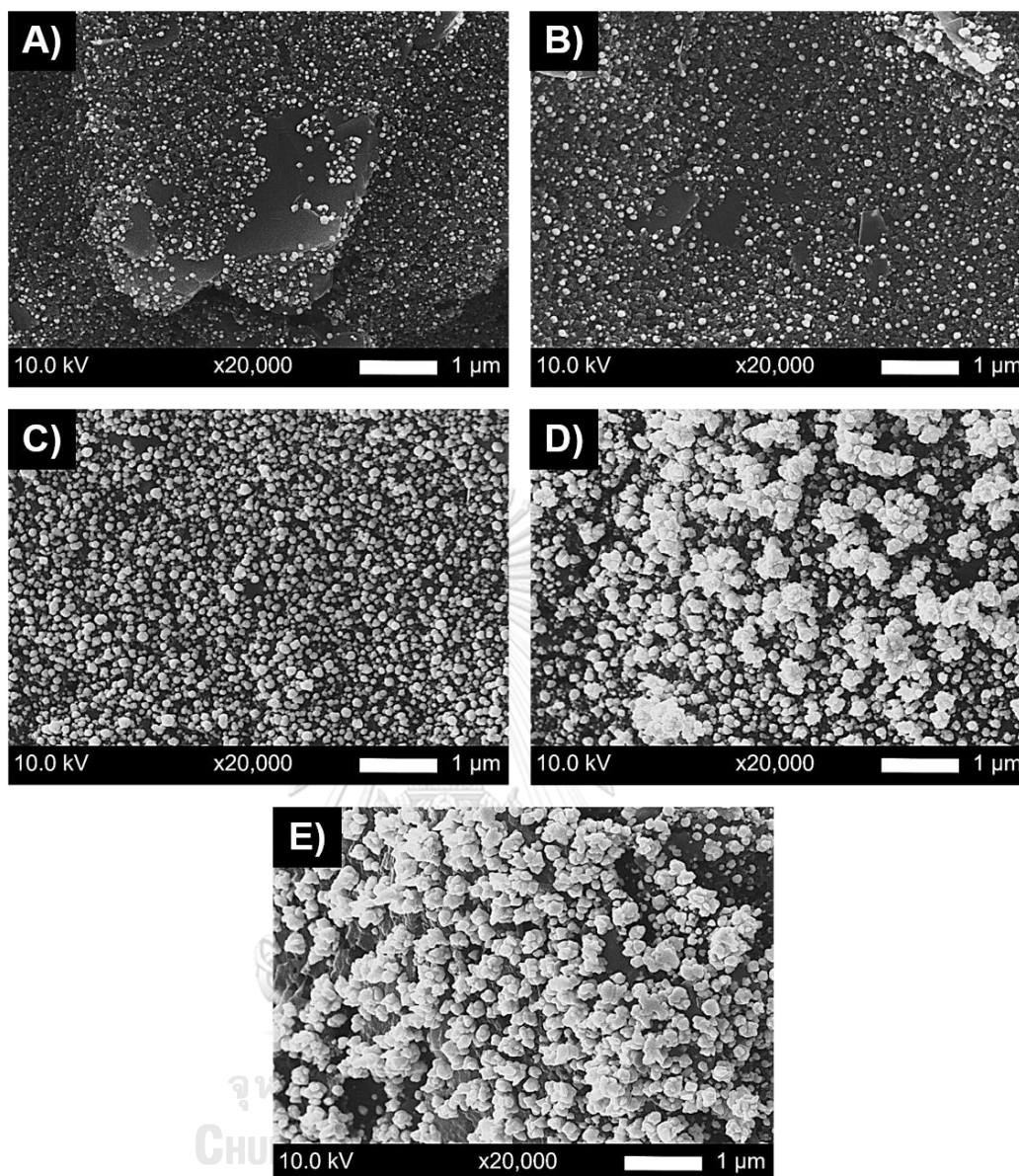
Figure 4.9 SEM images of the AuNPs/carbon-coated cotton thread with different electrodeposition time, (A) 30 s, (B) 60 s, (C) 120 s, (D) 180 s and (E) 240 s with magnification of 20,000×.

4.4 Optimization of parameters for uric acid detection

To obtain the high electrochemical sensitivity of the developed sensor for the detection of UA by DPV, the electrochemical parameters including step potential, amplitude and pulse width were systematically optimized by measuring of 1.0 mM UA in 0.1 M PBS on the modified cotton thread-based sensor. The selection of optimal conditions was based on the high current response along with the narrow

peak with symmetry. The results showed the highest anodic peak current response at 15 mV of the step potential (Figure 4.10), 200 mV of the amplitude (Figure 4.11) and 50 mV of the pulse width (Figure 4.12). At the higher step potential, amplitude and pulse width, the anodic peak current responses decreased due to broader peak shape. Therefore, a step potential of 15 mV, an amplitude of 200 mV and a pulse width of 50 ms were selected for the detection of UA in this study.

จุฬาลงกรณ์มหาวิทยาลัย
CHULALONGKORN UNIVERSITY
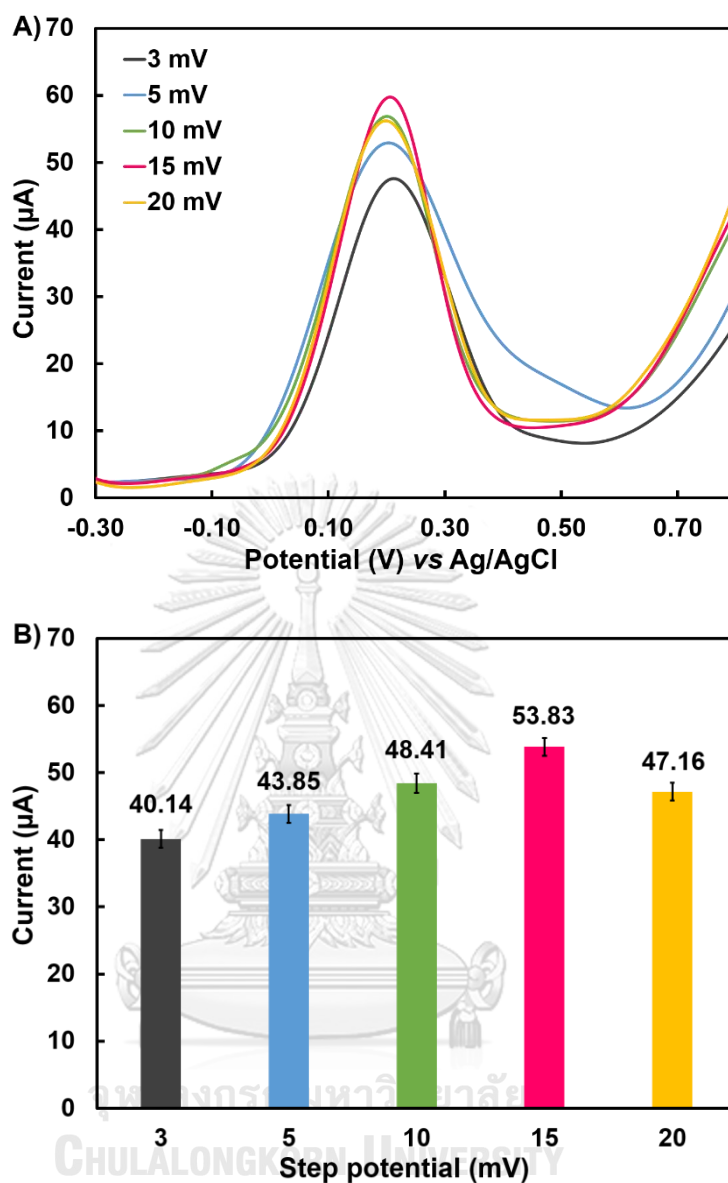
Figure 4.10 (A) Differential pulse voltammograms of 1.0 mM uric acid using the modified cotton thread-based sensor with different step potentials (3, 5, 10, 15 and 20 mV) and (B) anodic peak currents obtained from differential pulse voltammograms in Figure 4.10A.
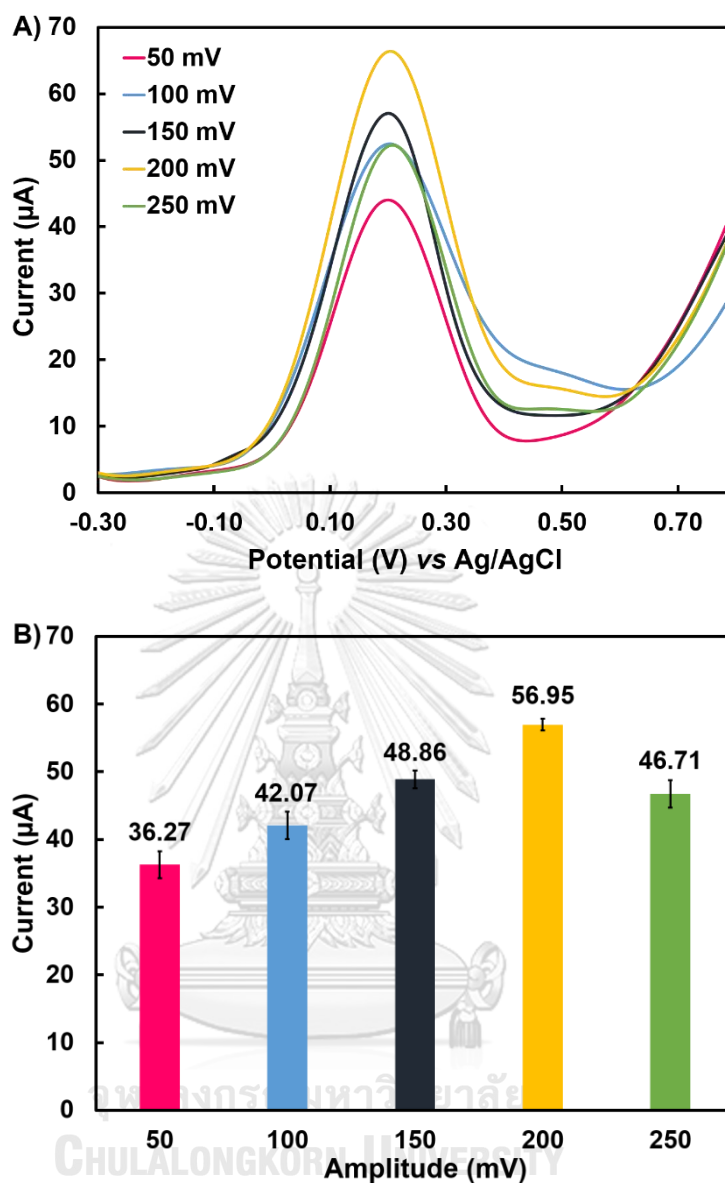
Figure 4.11 (A) Differential pulse voltammograms of 1.0 mM uric acid using the modified cotton thread-based sensor with different amplitudes (50, 100, 150, 200 and 250 mV) and (B) anodic peak currents obtained from differential pulse voltammograms in Figure 4.11A.
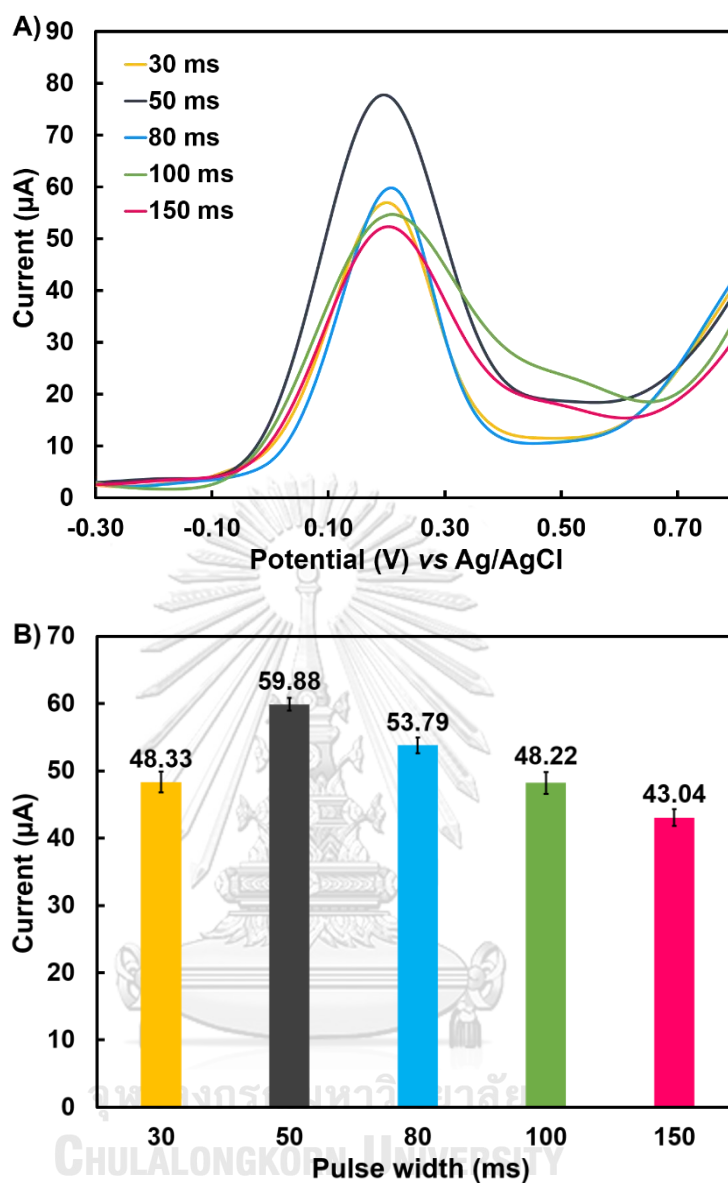
Figure 4.12 (A) Differential pulse voltammograms of 1.0 mM uric acid using the modified cotton thread-based sensor with pulse widths (30, 50, 80, 100 and 150 mV) and (B) anodic peak currents obtained from differential pulse voltammograms in Figure 4.12A.

4.5 The analytical performances of the cotton thread-based electrochemical sensor

The analytical performances of the developed cotton thread-based sensor towards UA detection were also investigated by DPV. As shown in Figure 4.13A, the anodic peak current linearly increased with the increasing of UA concentrations

ranging from 0.01 mM to 5.0 mM and a calibration curve between current (μA) and UA concentration (mM) was plotted in Figure 4.13B. The linear ranges of UA were observed from 0.01—0.5 mM (Figure 4.14A) and 0.5—5.0 mM (Figure 4.14B) with correlation coefficients (R^2) of 0.9975 and 0.9987, respectively. The limit of detection (LOD) was obtained by calculation using the following equation; LOD=3S/N, where S is a standard deviation of a signal obtained from a blank solution (*n*=7), N is a slope of calibration curve. The LOD was found to be 0.12 μM indicating that the developed sensor was sensitively enough for the determination of UA in human urine.
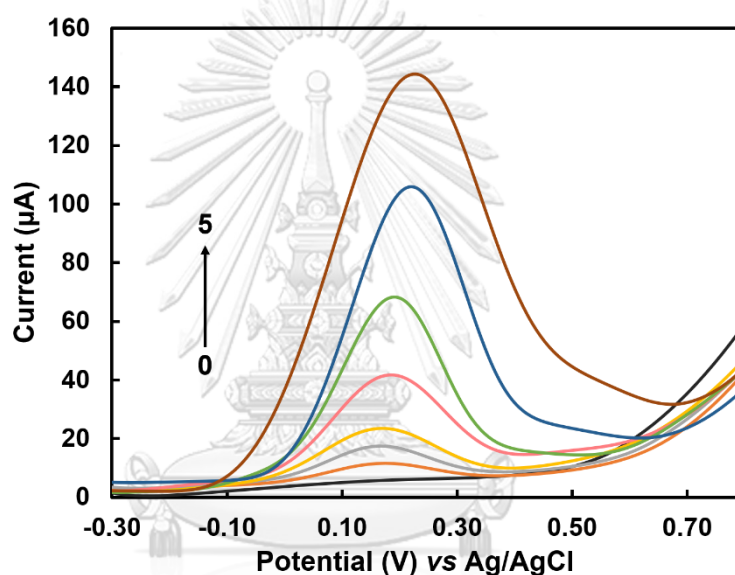
Figure 4.13 Differential pulse voltammograms of different concentrations of UA (0—5 mM) on the modified cotton thread-based sensor.
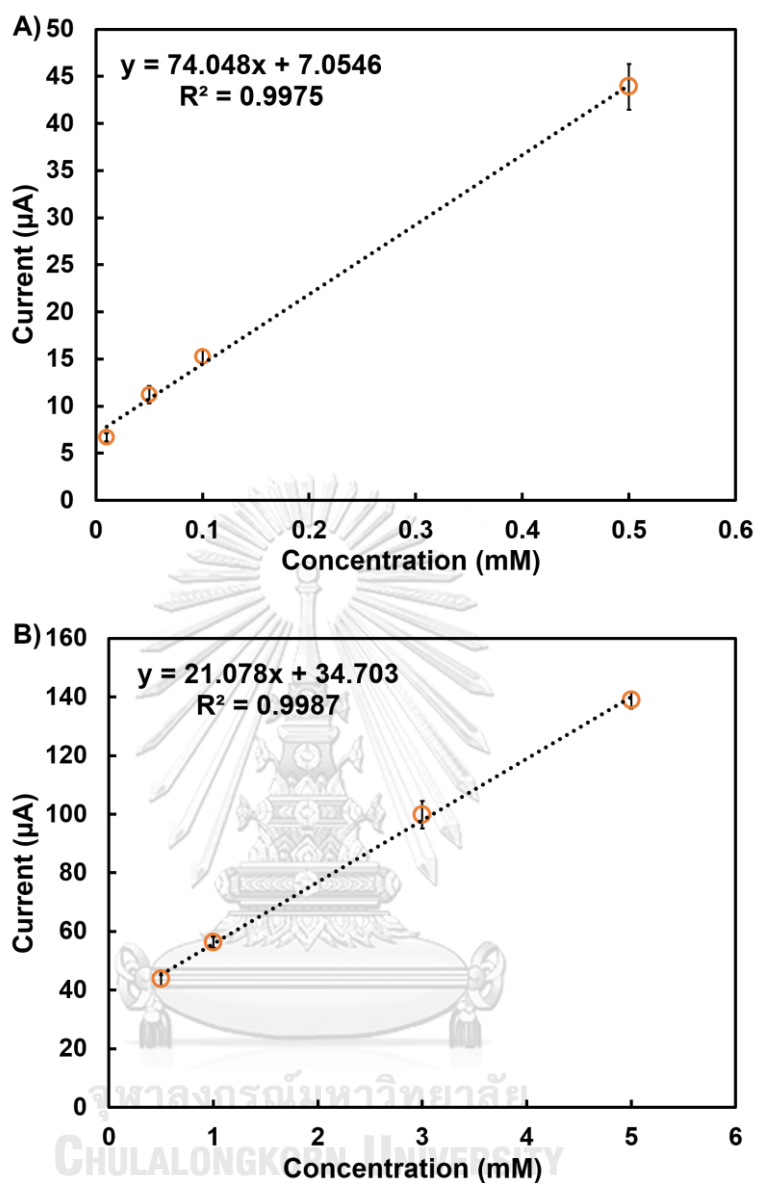
Figure 4.14 The linearities of UA detection at different concentrations from (A) 0.01—0.5 mM and (B) 0.5—5.0 mM.

Linear ranges and LOD for UA detection in this work were comparable with previous works, as summarized in Table 4.1. The developed sensor provided lower LOD and wider linear range than previous works without the use of enzyme. These comparisons exhibited the efficiency of the developed sensor that could be applied for the sensitive determination of UA in complex biological fluids.

Table 4.1 Comparison of non-enzymatic UA determination using different modified electrodes.

Chemically Modified electrode	Method	LOD (µM)	Linear range (µM)	Refs.
MoS$_2$ based flexible sensor	Amperometry	1.169	10—400	[60]
H-Fe$_3$O$_4$@C/GNS/GCE	DPV	0.41	1—100	[63]
RGO/poly-l-lysine/GCE	DPV	0.15	20—200	[64]
Poly (DPA)/SiO$_2$@Fe$_3$O$_4$/CPE	DPV	0.40	1.2—8.2	[61]
Au-Cu$_2$O/rGO/GCE	DPV	6.5	100—900	[49]
GNP/ITO	DPV	0.28	10—100	[65]
Pd/rGO/GCE	DPV	1.6	6—469.5	[66]
NiO-trGO/GCE	DPV	10	100—500	[67]
Tin-rGO/GCE	DPV	0.35	30—215	[68]
AuNPs/cotton thread-based sensor	DPV	0.12	10—5000	This work

Abbreviations: DPV, differential pulse voltammetry; MoS$_2$, molybdenum disulfide; H-Fe$_3$O$_4$, hallow magnetite; C, carbon; GNS, graphene oxide nanosheets; GCE, glassy carbon electrode; RGO, reduced graphene oxide; DPA, dipicolinic acid; CPE, carbon paste electrode; Cu$_2$O, cuprous oxide; GNP, graphene nanoplatelet; ITO, tin oxide electrode; Pd, palladium; NiO, nickel oxide; trGO, thermally reduced graphene oxide; Tin, titanium nitride; AuNPs, gold nanoparticles.

4.6 Interferent study

In this study, the anti-interference ability of the cotton thread-based sensor was assessed by adding various potential interfering substances existing in the real urine samples, including 10-fold excess of glucose, creatinine, KCl, NaCl, urea, 1-fold excess of ascorbic acid and 1% excess of BSA. As shown in Figure 4.15, there were no significant current changes in the presence of the interfering substances because the relative error was below ±5% for UA detection. Therefore, this developed sensor might be a promising tool for the determination of UA in urine. However, when the

concentration of the interferences was higher than these, the current responses decreased which was probably caused by obstructing UA oxidation on the cotton thread-based sensor by interference ions, especially BSA, which is a biomarker of kidney disease that can be significantly interfere UA detection in urine. Thus, prior to apply this sensor for UA detection in kidney disease patients, the specified sample pretreatment protocol might be carried out, such as using anti-BSA column pretreatment.
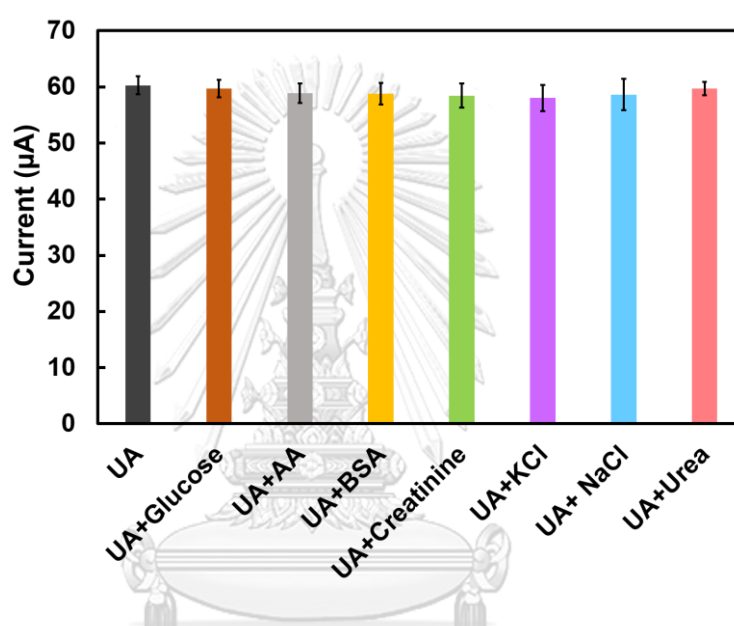
Figure 4.15 Current responses towards 1.0 mM UA on the cotton thread-based sensor in the presence and absence of several interferences.

4.7 Stability of the cotton thread-based sensor

The stability of the cotton thread-based sensor was investigating by measuring DPV response to 1.0 mM of UA in PBS solution multiple times. The modified cotton thread-based sensors were stored at room temperature for 30 days and the current responses remained above 96.5% of their initial values as shown in Figure 4.16. These results verified the good stability of the modified cotton thread-based sensors described in this study.
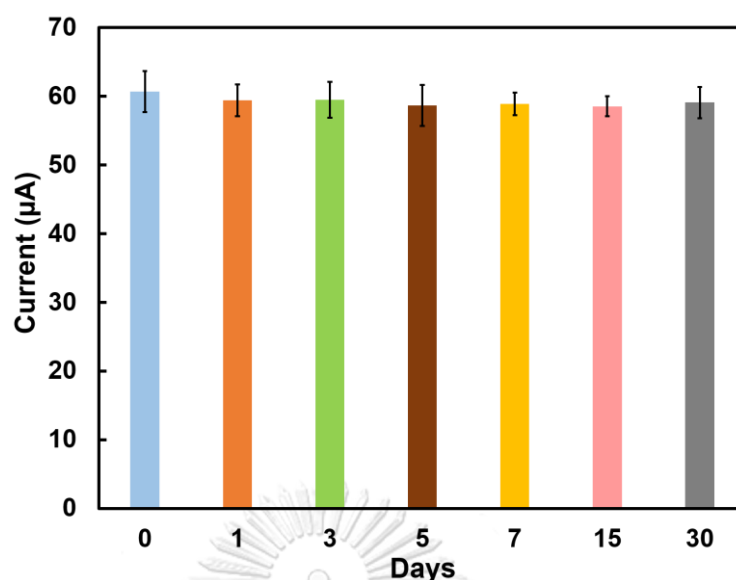
Figure 4.16 Stability of the modified cotton thread-based sensor with different periods after fabrication at room temperature.

4.8 Real sample analysis

To confirm the potential application of the modified cotton thread-based sensor in complex biological matrices, pooled urine sample was collected from 5 healthy adults (female). The use of pooled testing can significantly reduce the number of tests and verify the variety of samples with non-bias prior to medical diagnosis application. The urine sample was diluted with 0.1 M PBS solution, pH 6 (1:1), then the modified cotton thread-based sensor was used to detect UA in the samples using a standard addition method. The known amounts of UA (0.5, 1.0 and 2.0 mM) were added to the diluted sample and then were directly detected. The analytical results were summarized in Table 2. The recovery ranged from 101 to 108 and the relative standard derivation (RSD) (*n*=3) was below 6.0%, indicating that the modified cotton thread-based sensor has great potential for the detection of UA in real urine samples. As for the method validation, the results from LDI-MS were reported in Table 2, the similar concentrations were detected, verifying the high accuracy of this sensor.

Table 4.2 Determination of UA in human urine sample using the modified cotton thread-based sensor and LDI-MS.

Spiked UA concentration (mM)	Modified cotton thread-based sensor (mM)	Standard LDI-MS (mM)	Recovery (%)
Blank	0.61±0.08	0.70±0.09	—
0.5	1.11±0.02	1.17±0.05	104
1.0	1.69±0.05	1.73±0.07	101
2.0	2.77±0.12	2.84±0.15	107

จุฬาลงกรณ์มหาวิทยาลัย

CHULALONGKORN UNIVERSITY

CHAPTER V

CONCLUSION

5.1 Conclusion

In this study, the cotton thread-based electrochemical sensor was successfully fabricated and used for a non-invasive and non-enzymatic detection of uric acid (UA). The working electrode of the cotton thread-based sensor was coated by the carbon ink and then modified by AuNPs to increase the surface area and electrical conductivity leading to significant enhancement of the electrochemical sensitivity towards UA detection. The modification of AuNPs on the cotton thread-based sensor was performed by electrodeposition using 3.0 mM of chloroauric acid tetrahydrate (HAuCl$_4$) and 120 s of electrodeposition time as optimal values. For the detection of UA by DPV, a step potential of 15 mV, an amplitude of 200 mV and a pulse width of 50 ms were selected as the optimal electrochemical parameters.

Under the optimal conditions, calibration plot between UA concentration (mM) and the current (µA) response was observed with a linear range of 0.01 to 5.0 mM and LOD of 0.12 µM. This modified sensor displayed lower LOD and wider linear range than the previous reports. Furthermore, the sensor also presented 30 days of stability and anti-interference ability for various interfering substances existing in human urine. Eventually, this proposed system was successfully applied for the determination of UA in human urine with the recovery percentages from 101-107%.

5.2 Suggested works

This novel AuNPs modified cotton thread-based sensor might be an alternative tool for the non-invasive and non-enzymatic diagnosis of gout disease by measuring UA in urine obtained from the risk patients. Moreover, this sensor might be further integrated with the clothes, such as underwear by measuring UA in other fluids (*e.g.* sweat). Furthermore, this sensor might be further studied and applied for the non-invasive detection of other biomarkers.

REFERENCES

1. Doménech-Carbó, A., et al., *Electrochemical detection and screening of bladder cancer recurrence using direct electrochemical analysis of urine: A non-invasive tool for diagnosis.* Sensors and Actuators B: Chemical, 2018. **265**: p. 346-354.

2. Eftekhari, A., et al., *Bioassay of saliva proteins: The best alternative for conventional methods in non-invasive diagnosis of cancer.* Int J Biol Macromol, 2019. **124**: p. 1246-1255.

3. Michelena, J., et al., *Metabolomics Discloses a New Non-invasive Method for the Diagnosis and Prognosis of Patients with Alcoholic Hepatitis.* Ann Hepatol, 2019. **18**(1): p. 144-154.

4. Li, T., et al., *Non-invasive diagnosis of bladder cancer by detecting telomerase activity in human urine using hybridization chain reaction and dynamic light scattering.* Anal Chim Acta, 2019. **1065**: p. 90-97.

5. Ren, J., et al., *Environmentally-friendly conductive cotton fabric as flexible strain sensor based on hot press reduced graphene oxide.* Carbon, 2017. **111**: p. 622-630.

6. Promphet, N., et al., *Non-invasive textile based colorimetric sensor for the simultaneous detection of sweat pH and lactate.* Talanta, 2019. **192**: p. 424-430.

7. Weng, X., et al., *Recent advances in thread-based microfluidics for diagnostic applications.* Biosens Bioelectron, 2019. **132**: p. 171-185.

8. Polanský, R., et al., *A novel large-area embroidered temperature sensor based on an innovative hybrid resistive thread.* Sensors and Actuators A: Physical, 2017. **265**: p. 111-119.

9. Liu, P., et al., *Fully flexible strain sensor from core-spun elastic threads with integrated electrode and sensing cell based on conductive nanocomposite.* Composites Science and Technology, 2018. **159**: p. 42-49.

10. Oliveira, M.C., et al., *Nonenzymatic sensor for determination of glucose in blood plasma based on nickel oxyhydroxide in a microfluidic system of cotton*

thread. Journal of Electroanalytical Chemistry, 2019. **840**: p. 153-159.

11. Reches, M., et al., *Thread as a matrix for biomedical assays.* ACS Appl Mater Interfaces, 2010. **2**(6): p. 1722-8.

12. Ahmed, N.M., et al., *Single- and double-thread activated carbon fibers for pH sensing.* Materials Chemistry and Physics, 2019. **221**: p. 288-294.

13. Ford, E.S., et al., *Serum concentrations of uric acid and the metabolic syndrome among US children and adolescents.* Circulation, 2007. **115**(19): p. 2526-32.

14. Johnson, R.J., et al., *Is there a pathogenetic role for uric acid in hypertension and cardiovascular and renal disease?* Hypertension, 2003. **41**(6): p. 1183-90.

15. Liu, L., et al., *A novel electrochemical sensor based on bimetallic metal-organic framework-derived porous carbon for detection of uric acid.* Talanta, 2019. **199**: p. 478-484.

16. Bai, Z., et al., *Polyoxometalates-doped Au nanoparticles and reduced graphene oxide: A new material for the detection of uric acid in urine.* Sensors and Actuators B: Chemical, 2017. **243**: p. 361-371.

17. Li, X.L., et al., *Human nails metabolite analysis: A rapid and simple method for quantification of uric acid in human fingernail by high-performance liquid chromatography with UV-detection.* J Chromatogr B Analyt Technol Biomed Life Sci, 2015. **1002**: p. 394-8.

18. Pormsila, W., S. Krahenbuhl, and P.C. Hauser, *Capillary electrophoresis with contactless conductivity detection for uric acid determination in biological fluids.* Anal Chim Acta, 2009. **636**(2): p. 224-8.

19. Azmi, N.E., et al., *Fluorescence biosensor based on encapsulated quantum dots/enzymes/sol-gel for non-invasive detection of uric acid.* Journal of Luminescence, 2018. **202**: p. 309-315.

20. Han, B., et al., *Electrochemical Detection for Uric Acid Based on beta-Lactoglobulin-Functionalized Multiwall Carbon Nanotubes Synthesis with PtNPs Nanocomposite.* Materials (Basel), 2019. **12**(2).

21. da Cruz, F.S., et al., *Electrochemical detection of uric acid using graphite screen-printed electrodes modified with Prussian blue/poly(4-aminosalicylic*

acid)/Uricase. Journal of Electroanalytical Chemistry, 2017. **806**: p. 172-179.

22. Omar, M.N., et al., *Electrochemical detection of uric acid via uricase-immobilized graphene oxide.* Anal Biochem, 2016. **509**: p. 135-141.

23. Arora, K., M. Tomar, and V. Gupta, *Effect of processing parameters for electrocatalytic properties of SnO(2) thin film matrix for uric acid biosensor.* Analyst, 2014. **139**(4): p. 837-49.

24. Arora, K., M. Tomar, and V. Gupta, *Effect of processing parameters for electrocatalytic properties of SnO 2 thin film matrix for uric acid biosensor.* Analyst, 2014. **139**(4): p. 837-849.

25. Si, Y., et al., *Layer-by-layer electrochemical biosensors configuring xanthine oxidase and carbon nanotubes/graphene complexes for hypoxanthine and uric acid in human serum solutions.* Biosensors and Bioelectronics, 2018. **121**: p. 265-271.

26. Income, K., et al., *Disposable Nonenzymatic Uric Acid and Creatinine Sensors Using muPAD Coupled with Screen-Printed Reduced Graphene Oxide-Gold Nanocomposites.* Int J Anal Chem, 2019. **2019**: p. 3457247.

27. Wang, H., et al., *Rational Design of Gold Nanoparticle/graphene Hybrids for Simultaneous Electrochemical Determination of Ascorbic Acid, Dopamine and Uric Acid.* Chinese Journal of Analytical Chemistry, 2016. **44**(12): p. e1617-e1625.

28. Wang, Z., et al., *Simultaneous and selective measurement of dopamine and uric acid using glassy carbon electrodes modified with a complex of gold nanoparticles and multiwall carbon nanotubes.* Sensors and Actuators B: Chemical, 2018. **255**: p. 2069-2077.

29. Ji, D., et al., *Smartphone-based integrated voltammetry system for simultaneous detection of ascorbic acid, dopamine, and uric acid with graphene and gold nanoparticles modified screen-printed electrodes.* Biosens Bioelectron, 2018. **119**: p. 55-62.

30. Yukird, J., et al., *ZnO@graphene nanocomposite modified electrode for sensitive and simultaneous detection of Cd (II) and Pb (II).* Synthetic Metals, 2018. **245**: p. 251-259.

31. Bard, A.J. and L.R. Faulkner, *Fundamentals and applications.* Electrochemical

Methods, 2001. **2**(482): p. 580-632.

32.   Wang, J., *Analytical electrochemistry, 2nd edn Wiley*. 2000, VCH, New York.

33.   Kylberg, W., *Photo-electrochemical surface modification and analysis of dye sensitised solar cells*. 2008, University_of_Basel.

34.   Chemistry LibreTexts. *Mass transport mechanisms*. 2019, Jun 6; Available from: https://chem.libretexts.org/Bookshelves/Analytical_Chemistry/Supplemental_Modules_(Analytical_Chemistry)/Analytical_Sciences_Digital_Library/JASDL/Courseware/Analytical_Electrochemistry%3A_The_Basic_Concepts/03_Fundamentals_of_Electrochemistry/B%3A_The_Electrode_Process/03_Mass_Transport_Mechanisms.

35.   Tobias Owens. *Voltammetry and polarography*. 2018; Available from: https://slideplayer.com/slide/11831862/.

36.   Scientific Figure on ResearchGate. *Conducting polymer electrodes for thermogalvanic cells*. 2020, May 4; Available from: https://www.researchgate.net/figure/Cyclic-voltammogram-a-reversible-waveform-b-Quasi-reversible-waveform-and-c_fig22_329518660.

37.   Yifru, A., *Poly (3, 4–ethylenedioxythiophene)(PEDOT) Modified Glassy Carbon Electrode for the Voltammetric Determination of Diazinon*. 2010, Addis Ababa University.

38.   Seeber, R., C. Zanardi, and G. Inzelt, *The inherent coupling of charge transfer and mass transport processes: the curious electrochemical reversibility*. ChemTexts, 2016. **2**(2): p. 8.

39.   Catalano, J., *Manual Electrochemical Impedance Spectroscopy.* 2017.

40.   Luo, X., et al., *Application of Nanoparticles in Electrochemical Sensors and Biosensors.* Electroanalysis, 2006. **18**(4): p. 319-326.

41.   Ghosh, P., et al., *Gold nanoparticles in delivery applications.* Advanced drug delivery reviews, 2008. **60**(11): p. 1307-1315.

42.   Hu, G., et al., *Electrocatalytic oxidation and simultaneous determination of uric acid and ascorbic acid on the gold nanoparticles-modified glassy carbon electrode.* Electrochimica Acta, 2008. **53**(22): p. 6610-6615.

43.   Khater, M., et al., *Electrochemical detection of plant virus using gold*

nanoparticle-modified electrodes. Anal Chim Acta, 2019. **1046**: p. 123-131.

44. He, B. and H. Liu, *Electrochemical determination of nitrofuran residues at gold nanoparticles/graphene modified thin film gold electrode.* Microchemical Journal, 2019. **150**: p. 104108.

45. Hassani, S., et al., *Novel label-free electrochemical aptasensor for determination of Diazinon using gold nanoparticles-modified screen-printed gold electrode.* Biosens Bioelectron, 2018. **120**: p. 122-128.

46. Bernardo-Boongaling, V.R.R., et al., *Screen-printed electrodes modified with green-synthesized gold nanoparticles for the electrochemical determination of aminothiols.* Journal of Electroanalytical Chemistry, 2019. **847**: p. 113184.

47. Bandodkar, A.J. and J. Wang, *Non-invasive wearable electrochemical sensors: a review.* Trends in biotechnology, 2014. **32**(7): p. 363-371.

48. Rodgers, M.M., V.M. Pai, and R.S. Conroy, *Recent Advances in Wearable Sensors for Health Monitoring.* IEEE Sensors Journal, 2015. **15**(6): p. 3119-3126.

49. Aparna, T., R. Sivasubramanian, and M.A. Dar, *One-pot synthesis of Au-Cu2O/rGO nanocomposite based electrochemical sensor for selective and simultaneous detection of dopamine and uric acid.* Journal of Alloys and Compounds, 2018. **741**: p. 1130-1141.

50. Xuan, X., H.S. Yoon, and J.Y. Park, *A wearable electrochemical glucose sensor based on simple and low-cost fabrication supported micro-patterned reduced graphene oxide nanocomposite electrode on flexible substrate.* Biosensors and Bioelectronics, 2018. **109**: p. 75-82.

51. Jia, W., et al., *Electrochemical tattoo biosensors for real-time noninvasive lactate monitoring in human perspiration.* Anal Chem, 2013. **85**(14): p. 6553-60.

52. Bandodkar, A.J., et al., *Tattoo-based potentiometric ion-selective sensors for epidermal pH monitoring.* Analyst, 2013. **138**(1): p. 123-8.

53. Anastasova, S., et al., *A wearable multisensing patch for continuous sweat monitoring.* Biosens Bioelectron, 2017. **93**: p. 139-145.

54. Martin, A., et al., *Epidermal Microfluidic Electrochemical Detection System: Enhanced Sweat Sampling and Metabolite Detection.* ACS Sens, 2017. **2**(12): p. 1860-1868.

55. Liu, X. and P.B. Lillehoj, *Embroidered electrochemical sensors on gauze for rapid quantification of wound biomarkers.* Biosens Bioelectron, 2017. **98**: p. 189-194.

56. Gaines, M., et al., *A microfluidic glucose sensor incorporating a novel thread-based electrode system.* Electrophoresis, 2018. **39**(16): p. 2131-2135.

57. Kutzing, M.K. and B.L. Firestein, *Altered uric acid levels and disease states.* Journal of Pharmacology and Experimental Therapeutics, 2008. **324**(1): p. 1-7.

58. So, A. and B. Thorens, *Uric acid transport and disease.* The Journal of clinical investigation, 2010. **120**(6): p. 1791-1799.

59. Liu, L., et al., *A novel electrochemical sensor based on bimetallic metal–organic framework-derived porous carbon for detection of uric acid.* Talanta, 2019. **199**: p. 478-484.

60. Sha, R., N. Vishnu, and S. Badhulika, *MoS2 based ultra-low-cost, flexible, non-enzymatic and non-invasive electrochemical sensor for highly selective detection of uric acid in human urine samples.* Sensors and Actuators B: Chemical, 2019. **279**: p. 53-60.

61. Reddy, Y.V.M., et al., *Electrochemical sensor for detection of uric acid in the presence of ascorbic acid and dopamine using the poly (DPA)/SiO2@ Fe3O4 modified carbon paste electrode.* Journal of Electroanalytical Chemistry, 2018. **820**: p. 168-175.

62. Charoenkitamorn, K., O. Chailapakul, and W. Siangproh, *Development of gold nanoparticles modified screen-printed carbon electrode for the analysis of thiram, disulfiram and their derivative in food using ultra-high performance liquid chromatography.* Talanta, 2015. **132**: p. 416-423.

63. Song, H., et al., *Simultaneous voltammetric determination of dopamine and uric acid using carbon-encapsulated hollow Fe 3 O 4 nanoparticles anchored to an electrode modified with nanosheets of reduced graphene oxide.* Microchimica Acta, 2017. **184**(3): p. 843-853.

64. Zhang, D., et al., *Electrodeposited reduced graphene oxide incorporating polymerization of l-lysine on electrode surface and its application in*

simultaneous electrochemical determination of ascorbic acid, dopamine and uric acid. Materials Science and Engineering: C, 2017. **70**: p. 241-249.

65. Rahman, M.M., et al., *Highly sensitive and simultaneous detection of dopamine and uric acid at graphene nanoplatelet-modified fluorine-doped tin oxide electrode in the presence of ascorbic acid.* Journal of Electroanalytical Chemistry, 2017. **792**: p. 54-60.

66. Wang, J., et al., *Dopamine and uric acid electrochemical sensor based on a glassy carbon electrode modified with cubic Pd and reduced graphene oxide nanocomposite.* Journal of colloid and interface science, 2017. **497**: p. 172-180.

67. Aparna, T. and R. Sivasubramanian, *A facile hydrothermal synthesis of three dimensional flower-like NiO-thermally reduced graphene oxide (trGO) nanocomposite for selective determination of dopamine in presence of uric acid and ascorbic acid.* Journal of nanoscience and nanotechnology, 2018. **18**(2): p. 789-797.

68. Feng, J., et al., *Electrochemical detection mechanism of dopamine and uric acid on titanium nitride-reduced graphene oxide composite with and without ascorbic acid.* Sensors and Actuators B: Chemical, 2019. **298**: p. 126872.

VITA

NAME	Kanyapat Teekayupak
DATE OF BIRTH	20 March 1995
PLACE OF BIRTH	Bangkok, Thailand
INSTITUTIONS ATTENDED	B. Sc. in Chemistry, Faculty of Science, King Mongkut's University of Technology Thonburi, Bangkok, Thailand
HOME ADDRESS	234/172 IDEO sukhumvit 115, Sukhumvit Road, Theparak Sub-district, Muang District, Samutprakan, 10270
PUBLICATION	Kanyapat Teekayupak, Nipapan Ruecha, Nadnudda Rodthongkum, Orawon Chailapakul " Thread Based Wearable Electrochemical Sensor for Uric Acid Detection" Proceeding of Pure and Applied chemistry International Conference 2019, BITEC, Bangkok, Thailand, February 7-8, 2019, pp AC8-14.